

Energy-based Proportional Fairness in Cooperative Edge Computing

Thai T. Vu^{†‡}, Dinh Thai Hoang[†], Khoa T. Phan[‡], Diep N. Nguyen[†], and Eryk Dutkiewicz[†]

[†]School of Electrical and Data Engineering, University of Technology Sydney, Australia

[‡]Department of Computer Science and Information Technology, La Trobe University, Melbourne Australia

Abstract—By executing offloaded tasks from mobile users, edge computing augments mobile devices with computing/communications resources from edge nodes (ENs), enabling new services/applications (e.g., real-time gaming, virtual/augmented reality). However, despite being more resourceful than mobile devices, allocating ENs' computing/communications resources to a given favorable set of users (e.g., closer to edge nodes) may block other devices from their service. This is often the case for most existing task offloading and resource allocation approaches that only aim to maximize the network social welfare or minimize the total energy consumption but do not consider the computing/battery status of each mobile device. This work develops an energy-based proportional fair task offloading and resource allocation framework for a multi-layer cooperative edge computing network to serve all user equipments (UEs) while considering both their service requirements and individual energy/battery levels. The resulting optimization involves both binary (offloading decisions) and real variables (resource allocations). To tackle the resulting NP-hard mixed integer optimization problem, we leverage the fact that the relaxed problem is convex and propose a distributed algorithm, namely the dynamic branch-and-bound Benders decomposition (DBBD). DBBD decomposes the original problem into a master problem (MP) for the offloading decisions and multiple subproblems (SPs) for resource allocation. To quickly eliminate inefficient offloading solutions, the MP is integrated with powerful Benders cuts exploiting the ENs' resource constraints. We then develop a dynamic branch-and-bound algorithm (DBB) to efficiently solve the MP considering the load balance among ENs. The SPs can either be solved for their closed-form solutions or be solved in parallel at ENs, thus reducing the complexity. The numerical results show that the DBBD returns the optimal solution in maximizing the proportional fairness among UEs. The DBBD has higher fairness indexes, i.e., Jain's index and min-max ratio, in comparison with the existing ones that minimize the total consumed energy.

Keywords- Edge computing, offloading, resource allocation, fairness, energy efficiency, MINLP, branch-and-bound, Benders decomposition.

I. INTRODUCTION

Serving an ever-growing number of mobile user equipments (UEs) calls for novel network architectures, namely edge computing [1], [2]. In edge networks, edge nodes (ENs) are distributed closer to UEs to better serve high-demanding computing tasks, thus reducing the workload for backhaul links and enabling computation-demanding and low-latency services/applications (e.g., real-time gaming, augmented/virtual reality) [3]. However, while cloud servers, e.g., Amazon Web Services, often possess huge computing resources, an EN can provide limited computation services toward users due to its limited computing resources [4]. As such, the collaboration

among ENs as well as with cloud servers [5]–[12] to serve UEs has been considered as a very promising approach.

Moreover, offloading computing tasks from mobile devices to ENs is not always effective or even impossible due to the energy consumption for two-way data transmissions between the UEs and the ENs [1], [13] as well as tasks' security/QoS requirements. For that, the task offloading should be jointly optimized with the resource allocation. As aforementioned, despite being more resourceful than mobile devices, allocating ENs' limited computing/communications resources to a given favorable set of users may block one or other devices from their service. This is often the case for most existing task offloading and resource allocation approaches, e.g. [9], [12], [14]–[16], that only aim to maximize the network social welfare (e.g., optimizing the total consumed energy) but not consider the computing/battery status of each mobile device. Consequently, most resources are allocated to mobile devices/services with high marginal utilities. Whereas mobile devices, which have low marginal utilities, can be blocked from accessing ENs' resources. Therefore, fairness should be considered along with efficiency in edge computing.

A few recent works consider the fairness in resource allocation and task offloading in edge networks. The min-max cost policies or max-min energy balance are investigated in [5]–[8], [17]. For example, the work [8] aims to minimize the maximum delay among mobile devices. Other works, e.g., [18]–[20] consider fairness amongst ENs instead of user equipment. For instance, the work [20] develops an auction-aided scheme that enables fair bidding for communication resources between ENs in SDN-based ultra dense networks. We observe that the min-max/max-min policies only guarantee the upper bound of the cost function. They do not always provision the fairness among UEs since different UEs have different levels of resource demand. For example, it is unfair if the min-max policies are applied to two devices with 10 and 1 computational units, respectively. The work [21] accounts for the fairness amongst user vehicles and vehicle edge servers with a heuristic reward policy. Similarly, the authors of [22] introduce a heuristic scheme for computing resource allocation that can mitigate the effect of selfish mobile users. Lately, a few works investigate fairness [23], [24] using market equilibrium approaches. These papers rely on the game theory and market-based frameworks, which design the price for resources in a multiple edge node and budget-constrained buyer environment. However, the market-based framework is only applicable to the two-layer model (i.e., UEs and edge node layers) [23], [24]. Second, these approaches

cannot capture the coupling among different types of resources (i.e., the task duration depends on the uplink, downlink, and computation resources).

Given the above, this work develops an energy-based proportional-fair framework to serve all UEs with multiple tasks while considering both their service requirements and individual energy/battery levels in a multi-layer edge network architecture. Each UE, which may have multiple computing tasks, can connect to multiple nearby ENs to offload their tasks. The ENs can forward the tasks to a cloud server if they do not have sufficient resources to serve UEs. The edge computing and communication resources are to be jointly optimized with the task offloading decisions so as to fairly “share” the energy reduction/benefits (brought by the underlying edge network) to all UEs while taking into account the individual UEs’ energy/battery levels. The energy/battery level at each UE is captured via a nonnegative weight factor. To the best of our knowledge, this is the first work in the literature to address the fairness of energy benefit among users in a multi-layer edge computing system with multiple tasks.

The resulting problem for offloading tasks and allocating resources toward the tasks is a Mixed Integer Nonlinear Programming (MINLP), which is NP-hard [25]. Thus, solving the problem for its optimal solution is intractable. Consequently, most of the current researches in the literature either address small-scale problems or propose approximate algorithms to find sub-optimal solutions [5]–[11]. Although the main advantage of these approaches is low complexity in finding near-optimal solutions, there is no theoretical bound/guarantee on their solutions. Instead, this work aims to find the optimal solution of the problem with our practically low complexity approach. Specifically, we leverage the convexity of its relaxed problem to propose a distributed algorithm, namely the dynamic branch-and-bound Benders decomposition (DBBD). The DBBD decomposes the MINLP problem according to integer variables (offloading decisions) and real variables (resource allocations) into a master problem (MP) with integer variables and subproblems (SPs) with real variables at ENs. These subproblems can be solved iteratively and parallelly at ENs. We thus develop a dynamic branch-and-bound algorithm, namely DBB, which can effectively solve the MP considering the balance between the users’ demand and available resources at ENs. As a result, the optimal resource allocations amongst ENs, can be found at an early iteration of the DBBD. Besides, the DBB is designed so that the results from solving the MP are also reused between iterations of the DBBD, thus significantly reducing the solving time compared with the conventional branch-and-bound methods [12], [26]. The theoretical proofs and the numerical results confirm that the DBBD can always return the optimal solution maximizing the proportional fairness of the energy benefit among UEs, measured by Jain’s index and the min-max ratio [27]. The contributions of this paper are summarized as follows.

- An optimization joint task offloading and resource allocation problem is formulated to maximize the fairness of energy benefits amongst UEs in a multi-layer edge computing network, considering both UEs’ service requirements and ENs’ resource constraints.

- To address the resulting NP-hard MINLP problem, we develop an efficient dynamic branch-and-bound Benders decomposition (DBBD) to find the globally optimal solution. Specifically, applying the Benders decomposition approach to decouple the binary and real variables, the original problem is decomposed, respectively, into a master problem (MP) for offloading selection and subproblems (SPs) for communication and computation resource allocations. The MP and SPs are solved iteratively until obtaining the optimal solution that meets all requirements and constraints from both UEs and ENs. To support the DBBD, we develop a dynamic branch-and-bound algorithm (DBB) to dynamically pair computational tasks with the most potential EN, considering the tasks’ demand and available resources at ENs. Thus, the load balancing among ENs is also satisfied. Since the SPs are convex problems, a general optimizer is used to find the optimal resource allocations.
- We provide theoretical analysis to demonstrate and prove the optimality and the convergence of the proposed DBBD algorithm.
- The intensive numerical results confirm that the DBBD can always return the optimal solution maximizing the proportional fairness of the energy benefit among UEs, measured by Jain’s index and the min-max ratio [27]. We also provide comparisons with other benchmarks, e.g., FFBD, where the total energy consumption is minimized without considering the fairness [2], to show the outperformance of the proposed solution.

The rest of this paper is organized as follows. Section II describes the system model and problem formulation. In Section III, we introduce the proposed optimal solution. Section IV presents numerical results. Finally, Section V summarizes the major contributions and draws conclusions of this paper. The key notations used throughout the paper are summarized in Table I.

II. SYSTEM MODEL AND PROBLEM FORMULATION

A. System Model

Fig. 1 shows a three-layer edge computing system, including an edge layer with M edge nodes (ENs) $\mathcal{M} = \{1, \dots, M\}$, a cloud layer with one cloud server (CS), and a user layer with N user equipments (UEs) $\mathcal{N} = \{1, \dots, N\}$. Let $\mathbb{S} = \{1, \dots, S\}$ be the security levels of UEs, ENs, and the CS, in which 1 and S respectively denote the highest and lowest levels [4]. Let $\mathbb{Q} = \{1, \dots, Q\}$ be the application types of computational tasks. The security requirement of application type q is defined by a mapping $\Theta(q) \in \mathbb{S}$. UEs have a set of independent computational tasks, denoted by $\Phi = \cup_{n=1}^N \Phi_n$, in which Φ_n is the set of tasks at the UE n . These tasks can be executed locally at UEs, offloaded to either ENs or the CS for indirect transmission to the cloud via an EN or the cloud server V for direct transmission between UEs and the cloud. We have $\Phi_n \cap \Phi_m = \emptyset \ \forall n \neq m$ and $|\Phi| = \sum_{n=1}^N |\Phi_n|$. Here, $|\Phi|$ be the cardinality of set Φ . Each task I_i owned by UE $n \in \mathcal{N}$ can be defined by $I_i (L_i^u, L_i^d, w_i, t_i^r, s_i^r, q, n)$, in which L_i^u and L_i^d respectively are the input and output data size (in

TABLE I: List of key notations

Symbol	Physical meaning
\mathcal{N}	Set of user equipments (UEs)
\mathcal{M}	Set of edge nodes (ENs)
\mathcal{M}^*	$\mathcal{M} \cup \{\text{Cloud server } V\}$
\mathbb{Q}	Set of application types
\mathbb{S}	Set of security levels
$\mathbb{G}(q)$	Set of ENs that support application q
$\overline{\mathbb{G}}(q)$	Set of ENs that does not support application q
$\Psi_j \subseteq \mathbb{Q}$	Set of applications supported by EN j
Φ_n	Tasks of UE n belonging to Cat-3
$\hat{\Phi}_n$	Tasks of UE n belonging to Cat-4
Φ_n	$\hat{\Phi}_n \cup \Phi_n$, all tasks of UE n
$\hat{\Phi}$	$\bigcup_{n=1}^N \hat{\Phi}_n$, set of tasks belonging to Cat-3
$\hat{\Phi}$	$\bigcup_{n=1}^N \Phi_n$, set of tasks belonging to Cat-4
Φ	$\bigcup_{n=1}^N \Phi_n$, set of all tasks
Φ_j^t	Set of tasks offloaded to EN j in (SP ₁)
Φ_j^s	Set of tasks offloaded to cloud via EN j in (SP ₁)
Φ_j^{t+s}	$\Phi_j^t \cup \Phi_j^s$
$x_i^l, x_{ij}^d, x_{ij}^c$	Binary offloading variables determining if task I_i is processed locally, at EN j , or at cloud via EN j
\mathbf{x}_i	$(x_i^l, \{x_{ij}^d\}, \{x_{ij}^c\})$, $\forall i \in \mathcal{M}^*$
\mathbf{x}	$\{\mathbf{x}_i\}$, $\forall i \in \Phi$
$\mathbf{x}^{(k)}$	Offloading solution at iteration (k)
$r_{ij}^u, r_{ij}^d, r_{ij}^f$	Uplink, downlink, and CPU resource variables that EN j allocates to task I_i
\mathbf{r}_{ij}	$(r_{ij}^u, r_{ij}^d, r_{ij}^f)$
b_{ij}	Backhaul rate for transmitting task I_i between EN j and cloud
\mathbf{r}_j	$\{\mathbf{r}_{ij}\}$, $\forall i \in \Phi_j^{t+s}$
\mathbf{b}_j	$\{b_{ij}\}$, $\forall i \in \Phi_j^{t+s}$
(\mathbf{r}, \mathbf{b})	$(\{\mathbf{r}_{ij}\}, \{\mathbf{b}_{ij}\})$, $\forall (i, j) \in \Phi \times \mathcal{M}^*$
γ_j	Slack variable of (SP ₂)

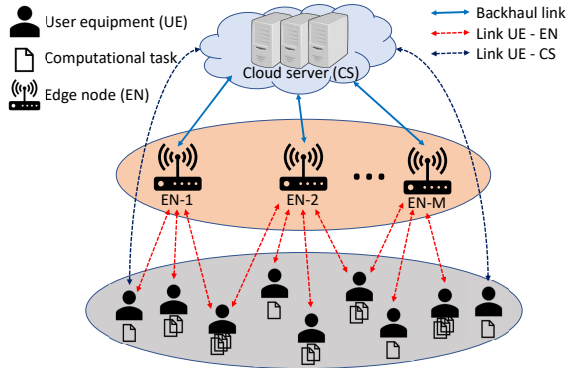


Fig. 1: Multi-layer edge computing system.

Mb), w_i is the number of required CPU Giga cycles per input data unit [8]. Thus, $L_i^u w_i$ is the required CPU Giga cycles of task I_i . The QoS of task I_i comprises the requirements of delay t_i^r and security $s_i^r = \Theta(q) \in \mathbb{S}$. The tasks can be processed only by UE n , ENs, or the CS satisfying their QoS.

1) *Local Processing*: The UE n has a security level $s_n^l \in \mathbb{S}$ and a CPU processing rate f_n^l . If the security requirement of task I_i can be met, i.e., $s_n^l \leq s_i^r$, then task I_i can be processed locally at UE n . As in [28]–[30], the chip architecture of UE n can define the CPU power consumption rate as $P_n^l = \alpha(f_n^l)^\gamma$ with its specific parameters α and γ . Commonly, $\alpha = 10^{-11}$ Watt/cycle $^\gamma$ and $\gamma = 2$ since the consumed energy per operation is proportional to the square

of the CPU's supply voltage, which is approximately linearly proportional to f_n^l [31]. The energy consumption E_i^l and the necessary computing time T_i^l of UE n are given by

$$E_i^l = P_n^l T_i^l = \alpha(f_n^l)^\gamma (L_i^u w_i) / f_n^l = \alpha(f_n^l)^{\gamma-1} (L_i^u w_i), \quad (1)$$

$$T_i^l = (L_i^u w_i) / f_n^l. \quad (2)$$

2) *Edge Node Processing*: Edge node j has capabilities defined by $(R_j^u, R_j^d, R_j^f, s_j^f, \Psi_j)$, where $R_j^u, R_j^d, R_j^f, s_j^f \in \mathbb{S}$, and $\Psi_j \subseteq \mathbb{Q}$ respectively are the total uplink, total downlink, the CPU cycle, its security level, and the set of applications supported by EN j .

If task I_i is offloaded and processed at EN j , then this node will allocate resources for the UE n , defined by $\mathbf{r}_{ij} = (r_{ij}^u, r_{ij}^d, r_{ij}^f)$, in which r_{ij}^u, r_{ij}^d are uplink/downlink rates for transmitting the input/output, and r_{ij}^f is the computing resource for executing the task. The UE n will consume an amount of energy for transmitting input data to and receiving output data from the EN j . The latency of task I_i comprises the time for transmission input/output and the task-execution time at EN j .

Let e_{ij}^u and e_{ij}^d be the consumed energy rates of transmitting and receiving data. Let ζ be the delay caused by multi-access. UE n has the consumed energy E_{ij}^f and the delay T_{ij}^f given by

$$E_{ij}^f = e_{ij}^u L_i^u + e_{ij}^d L_i^d, \quad (3)$$

$$T_{ij}^f = L_i^u / r_{ij}^u + L_i^d / r_{ij}^d + (L_i^u w_i) / r_{ij}^f + \zeta. \quad (4)$$

3) *Cloud Server Processing (offloaded via an edge node)*: Let $\mathcal{B} = \{\mathcal{B}_1, \dots, \mathcal{B}_M\} \in \mathbb{R}^M$ be the backhaul capacity between M ENs and the CS. All tasks offloaded to the CS via EN j will share the backhaul \mathcal{B}_j . Let $\mathcal{C} = \{\mathcal{C}_1, \dots, \mathcal{C}_Q\} \in \mathbb{R}^Q$ be the processing rate the CS can allocate to each task of Q applications. Let s_q^c be the security level of the CS toward application q . If the security requirement is satisfied, i.e., $s_i^r \geq s_q^c$, then EN j can forward task I_i to the CS.

In this case, the EN j will allocate resources $\mathbf{r}_{ij} = (r_{ij}^u, r_{ij}^d, r_{ij}^f)$ for the UE n , where r_{ij}^u, r_{ij}^d are uplink/downlink rates for transmitting input/output data, and $r_{ij}^f = 0$ (since it does not process the task). Then, the CS will allocate backhaul rate b_{ij} to transmitting input/output data between EN j and the CS. Task i will be processed at the CS with computation rate \mathcal{C}_q . The energy consumption E_{ij}^c at the UE includes the energy for transmitting/receiving input/output to and from EN j . The delay T_{ij}^c comprises the time for transmitting the input from the UE to the CS via FN j , the time for receiving the output from the CS via the EN j , and the time for executing the task at the CS. These metrics are given by

$$E_{ij}^c = E_{ij}^f = e_{ij}^u L_i^u + e_{ij}^d L_i^d, \quad (5)$$

$$T_{ij}^c = L_i^u / r_{ij}^u + L_i^d / r_{ij}^d + (L_i^u + L_i^d) / b_{ij} + (L_i^u w_i) / \mathcal{C}_q + \zeta. \quad (6)$$

4) *Cloud Server Processing (directly offloaded by user equipment)*: To simplify the notation, in the sequel we denote the cloud V as an extra edge node, i.e., $(M+1)$ -th EN, of the set $\mathcal{M}^* = \mathcal{M} \cup \{V\}$. All UEs share resources denoted by $(R_{(M+1)}^u, R_{(M+1)}^d, R_{(M+1)}^f, s_{(M+1)}^f, \Psi_{(M+1)})$ for the direct connection to the cloud. Here, $R_{(M+1)}^u, R_{(M+1)}^d$,

TABLE II: Categories of tasks according to energy benefits and QoS satisfaction.

Task Categories	Local QoS	Offloading QoS	Offloading Benefits	Pre-decision
Cat-1	✓	–	✗	pre-local
Cat-2	✓	✗	✓	pre-local
Cat-3 ($\hat{\Phi}$)	✓	✓	✓	local, offload
Cat-4 ($\tilde{\Phi}$)	✗	✓	–	offload

and $R_{(M+1)}^f$ are total uplink, downlink, and the CPU cycle of the cloud, respectively. The security level $s_{(M+1)}^f$ is defined as $s_{(M+1)}^f = s_q^c$ for the application type q and $\Psi_{(M+1)} = \mathbb{Q}$ shows that the cloud V can support all application types.

If task I_i is directly offloaded to the cloud V (or the $(M+1)$ -th node) for execution, the cloud will allocate uplink/downlink communication and computation resources toward UE n , denoted $\mathbf{r}_{i(M+1)} = (r_{i(M+1)}^u, r_{i(M+1)}^d, r_{i(M+1)}^f)$, for input/output transmission and executing the task. In this case, the consumed energy of the UE $E_{i(M+1)}^f$ and the delay $T_{i(M+1)}^f$ are similar to those in Eqs. (3) and (4) and given by

$$E_{i(M+1)}^f = e_{i(M+1)}^u L_i^u + e_{i(M+1)}^d L_i^d, \quad (7)$$

$$T_{i(M+1)}^f = L_i^u / r_{i(M+1)}^u + L_i^d / r_{i(M+1)}^d + (L_i^u w_i) / r_{i(M+1)}^f + \zeta, \quad (8)$$

where $e_{i(M+1)}^u$ and $e_{i(M+1)}^d$ are the energy consumption for directly transmitting and receiving a unit of data between the UE n and the cloud.

Since the cloud (i.e., $(M+1)$ th node) is the top layer, it cannot forward the task to a higher layer. Mathematically, this is captured by setting the backhaul capacity to the higher layer $\mathcal{B}_{(M+1)} = 0$.

5) *Task Categorization*: If processing a computational task requires less energy than the worst case (i.e., local processing or the worst case of offloading), then we say it has energy benefits. This work aims to maximize the fairness in terms of energy benefits amongst the devices when processing their tasks. From Eqs. (1), (3), (5), and (7), we can detect tasks to be either processed locally or offloaded according to the QoS satisfaction and energy benefits at local devices and from offloading. Thus, we define four categories of tasks as in Table II. This is the preparatory step before solving the problem. For the tasks in **Cat-1** and **Cat-2**, while local execution satisfies the QoS requirements, the offloading does not lead to the energy benefits and the QoS satisfaction, respectively, thus they are predetermined to be processed locally. For the tasks in **Cat-3**, the QoS requirements are satisfied by both local processing and offloading. Thus, depending on the available resources at ENs and the cloud, the tasks can be either processed locally or offloaded. For the tasks in **Cat-4**, only offloading satisfies their QoS requirements, thus they are predetermined to be offloaded. In this paper, we do not consider tasks that neither local processing nor offloading meets their QoS requirements.

Since computational tasks in **Cat-1** and **Cat-2** are predetermined to be processed locally, without loss of generality, we assume that Φ contains computational tasks only belonging to **Cat-3** and **Cat-4**, denoted $\hat{\Phi}$ and $\tilde{\Phi}$, respectively. Equivalently,

for UE n , let $\hat{\Phi}_n$ and $\tilde{\Phi}_n$ respectively be the sets of its tasks belonging to **Cat-3** and **Cat-4**. Thus, we have $\Phi = \hat{\Phi} \cup \tilde{\Phi}$ and $\Phi_n = \hat{\Phi}_n \cup \tilde{\Phi}_n$.

B. Problem Formulation

The offloading decisions of task I_i can be modelled as $\mathbf{x}_i = (x_i^l, x_{i1}^f, \dots, x_{i(M+1)}^f, x_{i1}^c, \dots, x_{i(M+1)}^c)$, where either $x_i^l = 1$ or $x_{ij}^f = 1$ or $x_{ij}^c = 1$ determines that task I_i is exclusively executed at either the UE or EN j or the CS (via EN j). Equivalently, we have the delay and energy consumption, i.e., $\mathbf{h}_i = (T_i^l, T_{i1}^f, \dots, T_{i(M+1)}^f, T_{i1}^c, \dots, T_{i(M+1)}^c)$ and $\mathbf{e}_i = (E_i^l, E_{i1}^f, \dots, E_{i(M+1)}^f, E_{i1}^c, \dots, E_{i(M+1)}^c)$, as in Eqs. (1)–(8).

Due to either the energy, the computing limitations, or the security requirements, not all tasks can be processed locally (e.g., local processing cannot satisfy the delay requirement). For that, we classify the set of tasks Φ into two categories: $\hat{\Phi}$ for tasks that can be either executed locally or offloaded and $\tilde{\Phi}$ for tasks that are unable to be executed locally but always need to be offloaded.

Let E_i^{base} denote the total energy consumption required for the *baseline solution* to execute task I_i , depending on which category the task belongs to. Recall that we only consider two categories of tasks, i.e., **Cat-3** and **Cat-4**, which are respectively denoted by $\hat{\Phi}$ and $\tilde{\Phi}$ as in Section II-A5. For the case that task $I_i \in \tilde{\Phi}$, which always needs to be offloaded, we have $E_i^{base} = \max_{j \leq (M+1)} \{E_{ij}^f, E_{ij}^c\} = \max_{j \leq (M+1)} \{E_{ij}^f\}$ since $E_{ij}^c = E_{ij}^f$ as in Eq. (5). For the case that task $I_i \in \hat{\Phi}$, which can be processed locally or offloaded, we have $E_i^{base} = E_i^l$. Thus, we can define E_i^{base} as

$$E_i^{base} = \begin{cases} E_i^l, & I_i \in \hat{\Phi}, \\ \max_{j \leq (M+1)} \{E_{ij}^f, E_{ij}^c\} = \max_{j \leq (M+1)} \{E_{ij}^f\}, & I_i \in \tilde{\Phi}. \end{cases} \quad (9)$$

As aforementioned, \mathbf{e}_i and \mathbf{h}_i are the energy consumption and the delay, corresponding to the offloading decisions \mathbf{x}_i . The energy benefit/saving Δ_i of UE in comparing with the base line E_i^{base} and the task-execution delay T_i are given by

$$\Delta_i = (E_i^{base} - \mathbf{e}_i)^\top \mathbf{x}_i, \quad (10)$$

$$T_i = \mathbf{h}_i^\top \mathbf{x}_i, \quad (11)$$

The relaxation of T_i in Eq. (11) is not convex due to its factors of the form x/r where x and r are the offloading decision and resource allocation variables. The Hessian of x/r is $\mathbf{H} = \begin{bmatrix} 0 & -\frac{1}{r^2} \\ -\frac{1}{r^2} & \frac{2x}{r^3} \end{bmatrix}$. \mathbf{H} is indefinite since $\det(\mathbf{H}) = -\frac{1}{r^4} < 0$. Thus, the expression x/r in T_i in Eq. (11) is neither convex or concave. Consequently, the optimization problem with the delay constraints, i.e., $T_i \leq t_i^r$, is not convex. To leverage convexity in finding the optimal solution, we transform T_i in Eq. (11) to an equivalent convex one. Let $\mathbf{y}_i = ((x_i^l)^2, (x_{i1}^f)^2, \dots, (x_{i(M+1)}^f)^2, (x_{i1}^c)^2, \dots, (x_{i(M+1)}^c)^2)$. We have $\mathbf{y}_i = \mathbf{x}_i$ due to its binary variables x_i^l , x_{ij}^f , and x_{ij}^c .

In the remainder of this paper, the delay T_i in Eq. (12) will be used for task I_i . We will prove its convexity in Theorem 1.

$$T_i = \mathbf{h}_i^\top \mathbf{y}_i, \quad (12)$$

Finally, we can define the utility function of the UE n with its set of computational tasks Φ_n as follows.

$$u_n = \sum_{I_i \in \Phi_n} \Delta_i. \quad (13)$$

The battery-equipped UEs often have limited energy, thus energy efficiency needs to be considered when processing their computational tasks. Without considering the fairness in energy reduction/benefit for users in the task offloading decision, one can simply optimize the total of all individual users' utility functions u_n in Eq. (13). As a result, the UEs owning the tasks with less energy benefit Δ_i may not be served from the offloading service. Consequently, these UEs will soon run out of energy and fail to maintain their functions. Unlike these works, e.g., [9], [12], [14]–[16], in the literature, this paper addresses a problem of jointly task-offloading (\mathbf{x}) and resource-allocating (\mathbf{r}, \mathbf{b}) = ($\{\mathbf{r}_{ij}\}, \{\mathbf{b}_{ij}\}$) so that all UEs can achieve their proportionally fair share of energy benefit/saving, considering their delay, security, application compatibility requirements as well as their battery/energy status. Let $\rho_n \in [0, 1]$ be the weight of the UE n that captures the user's battery status/priority level. Without loss of generality, we assume that $\forall n, \Phi_n$ is not empty and always has a task I_i with positive energy benefit, i.e., $\Delta_i > 0$. In other words, $u_n > 0, \forall n \in \mathcal{N}$.

According to the definition of proportional fairness in [32], a vector of utility functions $\mathbf{u} = (u_1, \dots, u_N)$ is **proportional fair**, if it is feasible, i.e., $\mathbf{u} \succ \mathbf{0}$ and the equivalent offloading and resource allocation solution satisfying task constraints. Here, \succ denotes componentwise inequality. In addition, for any other feasible vector \mathbf{u}^* regarding the proportional fairness over the weight ρ_n of each mobile device n , the aggregation of proportional changes is not positive as

$$\sum_{n=1}^N \rho_n \frac{u_n^* - u_n}{u_n} \leq 0. \quad (14)$$

Equivalently, Eq. (14) can be rewritten in the derivative form as follows.

$$\sum_{n=1}^N \rho_n (\ln(u_n))' du_n \leq 0. \quad (15)$$

From Eq. (15), the proportionally fair joint offloading and resource allocation solution can be obtained by maximizing of the utility function $\sum_{n=1}^N \rho_n \ln(u_n)$ over offloading decisions (\mathbf{x}) and resource allocation ($\mathbf{r} = \{\mathbf{r}_{ij}\}$ and $\mathbf{b} = \{\mathbf{b}_{ij}\}$) toward all tasks in $\Phi = \tilde{\Phi} \cup \hat{\Phi}$. The equivalent optimization problem considering tasks' QoS requirements and edge nodes' resource constraints is formally formulated as follows.

$$(\mathbf{P}_0) \quad \max_{\mathbf{x}, \mathbf{r}, \mathbf{b}} \sum_{n=1}^N \rho_n \ln(u_n), \text{ s.t.} \quad (16)$$

$$(\mathbf{R}_0) \quad \begin{cases} (\mathcal{C}_1) & T_i \leq t_i^r, \forall i \in \Phi, \\ (\mathcal{C}_2) & \sum_{i \in \Phi} r_{ij}^f \leq R_j^f, \forall j \in \mathcal{M}^*, \\ (\mathcal{C}_3) & \sum_{i \in \Phi} r_{ij}^u \leq R_j^u, \forall j \in \mathcal{M}^*, \\ (\mathcal{C}_4) & \sum_{i \in \Phi} r_{ij}^d \leq R_j^d, \forall j \in \mathcal{M}^*, \\ (\mathcal{C}_5) & \sum_{i \in \Phi} b_{ij} \leq \mathcal{B}_j, \forall j \in \mathcal{M}^*, \\ & r_{ij}^u, r_{ij}^d, r_{ij}^f, b_{ij} \geq 0, \forall (i, j) \in \Phi \times \mathcal{M}^*, \end{cases} \quad (17)$$

and

$$(\mathbf{X}_0) \quad \begin{cases} (\mathcal{C}_6) & x_i^l + \sum_{j=1}^{M+1} x_{ij}^f + \sum_{j=1}^{M+1} x_{ij}^c = 1, \forall i \in \Phi, \\ (\mathcal{C}_7) & x_i^l s_i^l + \sum_{j=1}^{M+1} x_{ij}^f s_j^f + \sum_{j=1}^{M+1} x_{ij}^c s_j^c \leq s_i^r, \forall i \in \Phi, \\ (\mathcal{C}_8) & x_{ij}^f = 0, \forall (i, j) \in \Phi \times \overline{\mathbb{G}}(q), \\ (\mathcal{C}_9) & x_i^l = 0, \forall i \in \tilde{\Phi}, \\ & x_i^l, x_{ij}^f, x_{ij}^c \in \{0, 1\}, \forall (i, j) \in \Phi \times \mathcal{M}^*, \end{cases} \quad (18)$$

where (\mathcal{C}_1) , (\mathcal{C}_7) , and (\mathcal{C}_8) capture tasks' QoS requirements, i.e., the delay, security, and application compatibility, (\mathcal{C}_2) , (\mathcal{C}_3) , (\mathcal{C}_4) , and (\mathcal{C}_5) capture ENs' resource bounds, i.e., the computational, uplink, downlink, and backhaul, (\mathcal{C}_6) constrains tasks' offloading decisions, and (\mathcal{C}_9) is the condition for tasks that are unable to be processed locally. $\overline{\mathbb{G}}(q)$ is the set of all ENs that do not support the application type q . As defined in Section II-A4, $\mathcal{M}^* = \mathcal{M} \cup \{V\}$.

III. PROPOSED OPTIMAL SOLUTIONS

As aforementioned, the MINLP optimization problem (\mathbf{P}_0) is NP-hard due to its binary (\mathbf{x}) and real variables (\mathbf{r}, \mathbf{b}). In general, it is intractable to find its optimal solution. However, by relaxing the integer variables to real numbers, the resulting relaxation of (\mathbf{P}_0) becomes a convex optimization problem [25]. In the sequel, we leverage this feature to develop an effective algorithm to find the optimal solution of (\mathbf{P}_0) .

A. Convexity of Relaxed Problem

From the original problem (\mathbf{P}_0) , we can transform it into a fully-relaxed problem as follows.

$$(\tilde{\mathbf{P}}_0) \quad \max_{\mathbf{x}, \mathbf{r}, \mathbf{b}} \sum_{n=1}^N \rho_n \ln(u_n), \text{ s.t. } (\mathbf{R}_0) \text{ and} \quad (19)$$

$$(\tilde{\mathbf{X}}_0) \quad \begin{cases} (\mathcal{C}_6) & x_i^l + \sum_{j=1}^{M+1} x_{ij}^f + \sum_{j=1}^{M+1} x_{ij}^c = 1, \forall i \in \Phi, \\ (\mathcal{C}_7) & x_i^l s_i^l + \sum_{j=1}^{M+1} x_{ij}^f s_j^f + \sum_{j=1}^{M+1} x_{ij}^c s_j^c \leq s_i^r, \forall i \in \Phi, \\ (\mathcal{C}_8) & x_{ij}^f = 0, \forall (i, j) \in \Phi \times \overline{\mathbb{G}}(q), \\ (\mathcal{C}_9) & x_i^l = 0, \forall i \in \tilde{\Phi}, \\ & x_i^l, x_{ij}^f, x_{ij}^c \in [0, 1], \forall (i, j) \in \Phi \times \mathcal{M}^*. \end{cases} \quad (20)$$

By converting all binary variables to real numbers, i.e., $x_i^l, x_{ij}^f, x_{ij}^c \in [0, 1], \forall (i, j) \in \Phi \times \mathcal{M}^*$, the resulting problem $(\tilde{\mathbf{P}}_0)$ is a standard nonlinear problem. Theorem 1 below proves the convexity of $(\tilde{\mathbf{P}}_0)$.

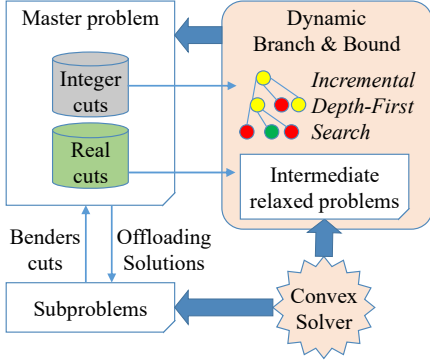


Fig. 2: Dynamic branch-and-bound Benders decomposition.

THEOREM 1. *The optimization problem $(\tilde{\mathbf{P}}_0)$ is convex.*

Proof: The proof is shown in Appendix A.

B. Dynamic Branch-and-Bound Benders Decomposition

We introduce a dynamic branch-and-bound Benders decomposition, namely DBBD, as in Fig. 2. In DBBD, (\mathbf{P}_0) is first decomposed according to integer variables (offloading decisions) and real variables (resource allocations) into a master problem (\mathbf{MP}_0) with the integer variables and subproblems (\mathbf{SP}_0) with the real variables. Then, we develop a dynamic branch-and-bound algorithm (DBB), which is equipped with an incremental depth-first search, to quickly find the optimal offloading solution of the (\mathbf{MP}_0) as in Fig. 2. The *Benders cuts* that eliminate inefficient solutions of (\mathbf{SP}_0) are generated and updated in the (\mathbf{MP}_0) . The DBBD finds the optimal solution of (\mathbf{P}_0) by iteratively solving (\mathbf{MP}_0) and (\mathbf{SP}_0) .

$$(\mathbf{MP}_0) \quad \mathbf{x}^{(k)} = \underset{\mathbf{x} \in \mathbf{X}_0}{\operatorname{argmax}} \left\{ \sum_{n=1}^N \rho_n \ln(u_n) \right\} \text{ s.t. } \text{cuts}^{(k)}, \quad (21)$$

$$(\mathbf{SP}_0) \quad \min_{\mathbf{r}, \mathbf{b} \in \mathbf{R}_0} \{0\}, \quad (22)$$

where $\text{cuts}^{(k)}$ is the set of Benders cuts generated at previous iterations $(1, \dots, (k-1))$ as in Section III-D, $\{0\}$ is the constant zero. Here, $\text{cuts}^{(k)}$ are constraints on offloading variables \mathbf{x} of (\mathbf{MP}_0) at iteration (k) .

In DBBD, at iteration (k) , (\mathbf{MP}_0) first is solved to find the offloading solution, i.e., $\mathbf{x}^{(k)}$, of (\mathbf{MP}_0) . Then, the (\mathbf{SP}_0) is solved to find the resource allocation, i.e., (\mathbf{r}, \mathbf{b}) , toward the offloaded tasks that are determined by $\mathbf{x}^{(k)}$ of (\mathbf{MP}_0) . According to Theorem 2, DBBD can terminate the iteration if either (\mathbf{MP}_0) is infeasible or it returns a solution $(\mathbf{x}, \mathbf{r}, \mathbf{b})$.

THEOREM 2. *At iteration (k) , if a solution (\mathbf{x}) of (\mathbf{MP}_0) leads to a solution (\mathbf{r}, \mathbf{b}) of (\mathbf{SP}_0) , then $(\mathbf{x}, \mathbf{r}, \mathbf{b})$ is the optimal one of (\mathbf{P}_0) . In addition, at iteration (k) , if (\mathbf{MP}_0) is infeasible, then (\mathbf{P}_0) is infeasible.*

Proof: The proof is shown in Appendix B.

C. Distributed Solving Subproblems

At iteration (k) , the offloading decision $\mathbf{x}^{(k)}$ helps to break down (\mathbf{SP}_0) into $(M+1)$ smaller independent problems

(\mathbf{SP}_1) at $(M+1)$ ENs (including the cloud server V). The resource allocation problem (\mathbf{SP}_1) at EN j is for tasks that are offloaded to EN j (denoted Φ_j^t) and to the CS via EN j (denoted Φ_j^s). Equivalently, these sets are captured by $\mathbf{x}_j^{f(k)} = (x_{1j}^f, \dots, x_{|\Phi_j^t|j}^f)^{(k)}$ and $\mathbf{x}_j^{c(k)} = (x_{1j}^c, \dots, x_{|\Phi_j^s|j}^c)^{(k)}$ in $\mathbf{x}^{(k)}$. Thus, we can define $\Phi_j^t = \{1, \dots, t\}$, $\Phi_j^s = \{t+1, \dots, t+s\}$, and $\Phi_j^{t+s} = \Phi_j^t \cup \Phi_j^s = \{1, \dots, t+s\}$ is captured by $\mathbf{x}_j^{(k)} = (\mathbf{x}_j^{f(k)}, \mathbf{x}_j^{c(k)})$. Variables $\mathbf{r}_j = (r_{1j}, \dots, r_{(t+s)j})$ and $\mathbf{b}_j = (b_{1j}, \dots, b_{(t+s)j})$ denote resource allocation of EN j towards the set of tasks Φ_j^{t+s} . The problem (\mathbf{SP}_1) at EN j can be defined as

$$(\mathbf{SP}_1) \quad \min_{\mathbf{r}_j, \mathbf{b}_j \in \mathbf{R}_j} \{0\}, \quad (23)$$

in which \mathbf{R}_j is the feasible region at EN j as follows.

$$(\mathbf{R}_j) \quad \begin{cases} (C_{1j}) & T_i \leq t_i^r, \forall i \in \Phi_j^{t+s}, \\ (C_{2j}) & \sum_{i \in \Phi_j^t} r_{ij}^f \leq R_j^f, \\ (C_{3j}) & \sum_{i \in \Phi_j^{t+s}} r_{ij}^u \leq R_j^u, \\ (C_{4j}) & \sum_{i \in \Phi_j^{t+s}} r_{ij}^d \leq R_j^d, \\ (C_{5j}) & \sum_{i \in \Phi_j^{t+s}} b_{ij} \leq B_j, \\ & r_{ij}^f, r_{ij}^u, r_{ij}^d, b_{ij} \geq 0, \forall i \in \Phi_j^{t+s}, \\ & r_{ij}^f = 0, \forall i \in \Phi_j^s, b_{ij} = 0, \forall i \in \Phi_j^t. \end{cases} \quad (24)$$

where (C_{1j}) captures the delay requirement of tasks, (C_{2j}) , (C_{3j}) , (C_{4j}) , and (C_{5j}) are the computational, uplink, downlink, and backhaul constraints of EN j .

Instead of directly solving (\mathbf{SP}_0) , the resource allocation solution can be found by parallelly solving $(M+1)$ smaller problems (\mathbf{SP}_1) at $(M+1)$ ENs in concurrence with the CS for (\mathbf{MP}_0) .

At iteration (k) , if $(M+1)$ subproblems (\mathbf{SP}_1) are feasible at all $(M+1)$ ENs, then $\mathbf{x}^{(k)}$, $\mathbf{r} = (\mathbf{r}_1, \dots, \mathbf{r}_{(M+1)})$, and $\mathbf{b} = (\mathbf{b}_1, \dots, \mathbf{b}_{(M+1)})$ are the optimal solutions of (\mathbf{P}_0) . Otherwise, for each infeasible (\mathbf{SP}_1) at EN j , a new Benders cut $c_j^{(k)}$, namely *Subproblem Benders Cut*, will be added to the cutting-plane set of (\mathbf{MP}_0) for the next iteration, i.e., $\text{cuts}^{(k+1)} = \text{cuts}^{(k)} \cup c_j^{(k)}$. These Benders cuts are designed in Section III-D1. To advance the efficiency of DBBD, we develop theoretical studies in the section below.

1) Feasibility and Infeasibility Detection: Replacing Eqs. (4), (6), and (8) into (C_{1j}) $T_i \leq t_i^r$ in (\mathbf{R}_j) of (\mathbf{SP}_1) , this delay constraint can be transformed as

$$\begin{cases} \left(\frac{L_i^u}{r_{ij}^u} + \frac{L_i^d}{r_{ij}^d} + \frac{L_i^u w_i}{r_{ij}^f} \right) \leq t_i^r - \zeta, & \forall i \in \Phi_j^t, \\ \left(\frac{L_i^u}{r_{ij}^u} + \frac{L_i^d}{r_{ij}^d} \right) + \left(\frac{L_i^u + L_i^d}{b_{ij}} \right) \leq t_i^r - \frac{L_i^u w_i}{C_q} - \zeta, & \forall i \in \Phi_j^s. \end{cases} \quad (25)$$

Remarkably, $(t_i^r - \zeta)$ and $(t_i^r - \frac{L_i^u w_i}{C_q} - \zeta)$ are constant components. If $\exists i \in \Phi_j^{t+s}$, $(t_i^r - \zeta) \leq 0$ or $(t_i^r - \frac{L_i^u w_i}{C_q} - \zeta) \leq 0$, then offloading task I_i to either EN j or the CS does not meet the delay requirement, i.e., $T_i \leq t_i^r$, leading to the infeasibility of (\mathbf{SP}_1) . In this case, a new cutting-plane is directly generated to prevent offloading task I_i . Otherwise, if $(t_i^r - \zeta) > 0, \forall i \in \Phi_j^t$ and $(t_i^r - \frac{L_i^u w_i}{C_q} - \zeta) > 0, \forall i \in \Phi_j^s$,

then the relative size, i.e., $(L_i^{u'}, L_i^{d'}, w_i', L_i^{c'})$, of task I_i is defined as

$$\begin{cases} \left(\frac{L_i^u}{t_i^u - \zeta}, \frac{L_i^d}{t_i^d - \zeta}, w_i, 0 \right), & \forall i \in \Phi_j^t \\ \left(\frac{L_i^u}{t_i^u - \frac{L_i^d w_i}{c_q} - \zeta}, \frac{L_i^d}{t_i^d - \frac{L_i^d w_i}{c_q} - \zeta}, 0, \frac{L_i^u + L_i^d}{t_i^u - \frac{L_i^d w_i}{c_q} - \zeta} \right), & \forall i \in \Phi_j^s. \end{cases} \quad (26)$$

For task I_i , let $\beta_i = \left(\frac{L_i^{u'}}{r_{ij}^u} + \frac{L_i^{d'}}{r_{ij}^d} + \frac{L_i^{u'} w_i'}{r_{ij}^f} + \frac{L_i^{c'}}{b_{ij}} \right)$. Then, the delay constraint in Eq. (25) becomes

$$\beta_i = \left(\frac{L_i^{u'}}{r_{ij}^u} + \frac{L_i^{d'}}{r_{ij}^d} + \frac{L_i^{u'} w_i'}{r_{ij}^f} + \frac{L_i^{c'}}{b_{ij}} \right) \leq 1, \forall i \in \Phi_j^{t+s}. \quad (27)$$

Based on the relative size concepts, Theorems 3 and 4 below, respectively, can detect the feasibility and the infeasibility of (\mathbf{SP}_1) .

THEOREM 3. Let $\beta_{bal}^u = \frac{\sum_{i \in \Phi_j^{t+s}} L_i^{u'}}{R_j^u}$, $\beta_{bal}^d = \frac{\sum_{i \in \Phi_j^{t+s}} L_i^{d'}}{R_j^d}$, $\beta_{bal}^f = \frac{\sum_{i \in \Phi_j^{t+s}} L_i^{u'} w_i'}{R_j^f}$, and $\beta_{bal}^b = \frac{\sum_{i \in \Phi_j^{t+s}} L_i^{c'}}{B_j}$. If $\beta_{bal} = \beta_{bal}^u + \beta_{bal}^d + \beta_{bal}^f + \beta_{bal}^b \leq 1$, then (\mathbf{SP}_1) is feasible and $\mathbf{r}_{ij} = (r_{ij}^u, r_{ij}^d, r_{ij}^f, b_{ij}) = (\frac{L_i^{u'}}{\beta_{bal}^u}, \frac{L_i^{d'}}{\beta_{bal}^d}, \frac{L_i^{u'} w_i'}{\beta_{bal}^f}, \frac{L_i^{c'}}{\beta_{bal}^b})$, $\forall i \in \Phi_j^{t+s}$, is a resource allocation solution.

Proof: The proof is shown in Appendix C.

THEOREM 4. If $\frac{\sum_{i \in \Phi_j^{t+s}} L_i^{u'}}{R_j^u} > 1$ or $\frac{\sum_{i \in \Phi_j^{t+s}} L_i^{d'}}{R_j^d} > 1$ or $\frac{\sum_{i \in \Phi_j^{t+s}} L_i^{u'} w_i'}{R_j^f} > 1$ or $\frac{\sum_{i \in \Phi_j^{t+s}} L_i^{c'}}{B_j} > 1$, then (\mathbf{SP}_1) is infeasible.

Proof: The proof is shown in Appendix D.

Theorem 3 can detect the closed-form resource allocation solutions of (\mathbf{SP}_1) at EN j without requiring an optimizer. As a result, the computation time is reduced. Similarly, Theorem 4 can quickly detect the infeasibility of (\mathbf{SP}_1) at EN j . However, we will exploit Theorem 4 in a more effective way by developing Benders cuts, namely *Resource Benders Cut*, for (\mathbf{MP}_0) to prevent the generation of (\mathbf{SP}_1) that violate Theorem 4. Those Benders cuts, presented in Section III-D2, will be added to the set *cuts* of (\mathbf{MP}_0) at the initial step of the DBBD. Consequently, a large number of useless offloading solutions are not generated, thus remarkably reducing the solving time of the DBBD.

2) *Optimizing the Delay Satisfaction Rate:* At EN j , the fairness in terms of delay is considered. Particularly, we solve (\mathbf{SP}_1) with the new form of delay constraint in Eq. (27) so that all tasks gain the same delay satisfaction rate γ_j . The solution of (\mathbf{SP}_1) , which minimizes the delay satisfaction rate γ_j , is equivalent to those of its variant problem (\mathbf{SP}_2) with an additional slack variable γ_j . Here, (\mathbf{SP}_2) is always feasible.

$$(\mathbf{SP}_2) \quad \min_{\mathbf{r}_j, \mathbf{b}_j, \gamma_j \in \mathbf{RZ}_j} \{\gamma_j\}, \quad (28)$$

where

$$(\mathbf{RZ}_j) \quad \begin{cases} (\mathcal{C}_{1j}) \quad \beta_i \leq \gamma_j, \forall i \in \Phi_j^{t+s}, \\ (\mathcal{C}_{2j}) \quad \sum_{i \in \Phi_j^t} r_{ij}^f \leq R_j^f, \\ (\mathcal{C}_{3j}) \quad \sum_{i \in \Phi_j^{t+s}} r_{ij}^u \leq R_j^u, \\ (\mathcal{C}_{4j}) \quad \sum_{i \in \Phi_j^{t+s}} r_{ij}^d \leq R_j^d, \\ (\mathcal{C}_{9j}) \quad \sum_{i \in \Phi_j^{t+s}} b_{ij} \leq B_j, \\ r_{ij}^f, r_{ij}^u, r_{ij}^d \geq 0, \forall i \in \Phi_j^{t+s}, \\ r_{ij}^f = 0, \forall i \in \Phi_j^s, \quad b_{ij} = 0, \forall i \in \Phi_j^t, \\ 0 < \gamma_j. \end{cases} \quad (29)$$

THEOREM 5. The optimization problem (\mathbf{SP}_2) is convex.

Proof: The proof is shown in Appendix E.

Due to the convexity of (\mathbf{SP}_2) , we can use an optimizer to find its optimal resource allocation solution. If (\mathbf{SP}_2) is feasible with the resulting delay satisfaction rate $\gamma_j \leq 1$, then (\mathbf{SP}_1) is feasible with the resource allocation solution of (\mathbf{SP}_2) . Otherwise, we conclude the infeasibility of (\mathbf{SP}_1) .

D. Benders Cut Generation

This section develops three types of Benders cuts, namely *Subproblem Benders Cut*, *Resource Benders Cut*, and *Prefixed-Decision Benders Cut*, that will be added to the constraints of (\mathbf{MP}_0) . Though the DBBD algorithm can find the optimal solution only by using the subproblem Benders cuts as presented below, the two other types of Benders cuts can help to reduce the search space, thereby significantly reducing the computation time of the algorithm. This approach is more advanced than that proposed in [33], in which only one Benders cut is updated at each iteration.

1) *Subproblem Benders Cut:* At iteration (k) , the problem (\mathbf{SP}_1) with assigned tasks Φ_j^{t+s} at EN j is determined by $\mathbf{x}_j^{(k)} = (\mathbf{x}_j^{f(k)}, \mathbf{x}_j^{c(k)})$. If (\mathbf{SP}_1) is infeasible, then a new Benders cut $c_j^{(k)}$ will be added to the *cuts* set of (\mathbf{MP}_0) to prevent offloading Φ_j^{t+s} in the next iterations.

$$c_j^{(k)} = \{\mathbf{x}_j^{f(k)\top} \mathbf{x}_j^f + \mathbf{x}_j^{c(k)\top} \mathbf{x}_j^c \leq t + s - 1\}. \quad (30)$$

2) *Resource Benders Cut:* To make a feasible problem (\mathbf{SP}_1) at EN j , the set $\Phi_j^{t+s} \subseteq \Phi$, which is determined by $(\mathbf{x}_j^f, \mathbf{x}_j^c)$, must not violate any resource constraints at EN j as presented in Theorem 4.

Let $\mathbf{c}_j^{u(edge)} = (L_1^{u'}, \dots, L_N^{u'})/R_j^u$, $\mathbf{c}_j^{d(edge)} = (L_1^{d'}, \dots, L_N^{d'})/R_j^d$ and $\mathbf{c}_j^{f(edge)} = (L_1^{u'} w_1', \dots, L_N^{u'} w_N')/R_j^f$. Here, $(L_i^{u'}, L_i^{d'}, w_i')$ is defined as in Eq. (26) for $i \in \Phi_j^t$.

Let $\mathbf{c}_j^{u(cloud)} = (L_1^{u'}, \dots, L_N^{u'})/R_j^u$, $\mathbf{c}_j^{d(cloud)} = (L_1^{d'}, \dots, L_N^{d'})/R_j^d$, and $\mathbf{c}_j^{b(cloud)} = (L_1^{c'}, \dots, L_N^{c'})/B_j$. Here, $(L_i^{u'}, L_i^{d'}, L_i^{c'})$ is defined as in Eq. (26) for $i \in \Phi_j^s$.

To avoid the infeasible conditions in Theorem 4, we need to add the cutting-planes below to the *cuts* set of (\mathbf{MP}_0) .

$$\begin{aligned} c_j^u &= \{\mathbf{c}_j^{u(edge)\top} \mathbf{x}_j^f + \mathbf{c}_j^{u(cloud)\top} \mathbf{x}_j^c \leq 1\}, \\ c_j^d &= \{\mathbf{c}_j^{d(edge)\top} \mathbf{x}_j^f + \mathbf{c}_j^{d(cloud)\top} \mathbf{x}_j^c \leq 1\}, \\ c_j^f &= \{\mathbf{c}_j^{f(edge)\top} \mathbf{x}_j^f \leq 1\}, \text{ and } c_j^b = \{\mathbf{c}_j^{b(cloud)\top} \mathbf{x}_j^c \leq 1\}. \end{aligned}$$

3) *Prefixed-Decision Benders Cut*: As aforementioned in Section III-C1, if $(t_i^r - \zeta) \leq 0$ and $(t_i^r - \frac{L_i^u w_i}{C_q} - \zeta) \leq 0$, then task I_i cannot be offloaded to ENs and the CS, respectively. Thus, suitable cutting-planes can be generated and updated in the *cuts* set of (\mathbf{MP}_0) . From Table II, we also can add suitable Benders cuts according to their pre-decisions.

E. Solving the Master Problem

Normally, branch-and-bound algorithms are often used to solve integer problems such as (\mathbf{MP}_0) . To support the DBBD, we thus develop a low-complexity dynamic branch-and-bound algorithm, namely DBB, that can efficiently solve (\mathbf{MP}_0) by exploiting the nature of binary decision variables as well as tasks' QoS requirements and ENs' available resources. Particularly, we first represent the computing offloading problem in the form of a decision tree. Each node on the tree is equivalent to a task, and the branches from that node are the possible processors (i.e., the UE, ENs, and the CS) toward the task. The computation/communication load of a branch is determined by the highest computation/communication load per processing unit amongst ENs/cloud. Then, the branches are arranged so that their load increases from left to right. Thus, a depth-first search will return the optimal solution satisfying the most load balancing amongst edge nodes and the cloud. In addition, an incremental search is implemented to speed up the optimal solution search processes by reusing the search results from the previous iterations (illustrated in Fig. 2). In the following, we introduce the structure of the decision tree, the incremental depth-first search, the dynamic task selection, and the balancing processor selection.

1) *Decision Tree of Tasks*: In the DBB algorithm, the decision tree has the following features.

- **Branching task**: Assume that each computational task has $(2(M+1)+1)$ offloading choices, including $(M+1)$ edge nodes, $(M+1)$ cloud servers (via $(M+1)$ edge nodes), and one local device. In practice, the number of possible offloading choices can be less than $(2(M+1)+1)$ due to QoS requirements (e.g., delay, security). Each node on the tree is equivalent to a task, and the branches from that node are the possible offloading choices for this task, forming a $(2(M+1)+1)$ -tree with the depth of $(|\Phi| - 1)$. The root node has a depth of 0.
- **Simplifying problem**: For the offloading variables x_i of task i , only one variable takes value 1, whereas all others take value 0 as in the offloading constraint (C_6) in Eq. (18). Thus, if $x_{ij}^f = 0$ (also $x_{ij}^c = 0$), we can remove all expressions of the forms $x_{ij}^f A$ (also $x_{ij}^c B$), and these variables in (\mathbf{MP}_0) . As a result, each node on the decision tree is also equivalent to an intermediate problem with fewer variables, namely (\mathbf{IP}) , in which the ancestor nodes have tasks with the fixed offloading decisions.
- **Preserving convexity**: Let $(\widetilde{\mathbf{MP}}_0)$ and $(\widetilde{\mathbf{IP}})$, respectively, be the relaxed problems of (\mathbf{MP}_0) and (\mathbf{IP}) . Due to the convexity of $(\widetilde{\mathbf{MP}}_0)$, the problem $(\widetilde{\mathbf{IP}})$, which is equivalent to $(\widetilde{\mathbf{MP}}_0)$ with some fixed offloading variables, is convex.

The low complexity of the DBB algorithm with the above characteristics compared with the standard branch-and-bound approach is evaluated in Section III-G.

2) *Incremental Depth-First Search*: If we consider all possible offloading policies as a search space, then the search space will be partitioned into subspaces by intermediate problems of the form (\mathbf{IP}) mentioned in Section III-E1. Here, we will introduce the incremental depth-first search (namely IDFS) to find the optimal offloading policy of (\mathbf{MP}) .

At iteration (k) , at a node of (\mathbf{IP}) on the tree, the result of the relaxed problem $(\widetilde{\mathbf{IP}})$ will be evaluated to determine the potential of having an optimal solution in that subspace. Then, a suitable action, i.e., branching or pruning, will be carried out. In the IDFS, at each node on the decision tree, the results from previous iterations will be evaluated so that a new search will be carried out on the sub-tree from that node only if it is an undiscovered potential subspace. Consequently, the solving time can be significantly reduced. There are two cases with the relaxed problem $(\widetilde{\mathbf{IP}})$ at iteration (k) as follows.

Case 1: If $(\widetilde{\mathbf{IP}})$ was feasible at previous iterations and the best result of both $(\widetilde{\mathbf{IP}})$ and (\mathbf{IP}) (if it exists) of previous iterations is not greater than that of the current optimal one, then we will prune the sub-tree starting from the node of (\mathbf{IP}) at the current iteration (k) , and the sub-tree will be stored for evaluation in future iterations.

Case 2: If either $(\widetilde{\mathbf{IP}})$ was not solved or $(\widetilde{\mathbf{IP}})$ was feasible at the previous iterations and the best result of both $(\widetilde{\mathbf{IP}})$ and (\mathbf{IP}) (if it exists) from previous iterations is greater than that of the current optimal one, then $(\widetilde{\mathbf{IP}})$ will be solved to determine the potential of having an optimal solution in that subspace. There are three possibilities when solving $(\widetilde{\mathbf{IP}})$ as below.

- If $(\widetilde{\mathbf{IP}})$ is infeasible, then we will prune the sub-tree starting from the node of (\mathbf{IP}) at the current iteration (k) and future iterations.
- If $(\widetilde{\mathbf{IP}})$ is feasible and the result is not better than that of the current optimal one, then we will prune the sub-tree starting from the node of (\mathbf{IP}) at the current iteration (k) , and the sub-tree will be stored for evaluation in future iterations.
- If $(\widetilde{\mathbf{IP}})$ is feasible and the result is better than that of the current optimal one, and if this node was not branched in previous iterations, we will choose a task to branch at this node as shown in Sections III-E3 and III-E4. The relaxed solution of $(\widetilde{\mathbf{IP}})$ will be updated as the current optimal if it is an integer solution.

In other words, the node of (\mathbf{IP}) will be pruned without solving if either $(\widetilde{\mathbf{IP}})$ is infeasible at any iteration or the best result of both (\mathbf{IP}) and $(\widetilde{\mathbf{IP}})$ from previous iterations is not better than that of the current optimal one. Since a large portion of the search space is pruned without resolving their intermediate problems, the overall solving time can be remarkably reduced.

To reuse results between iterations, the structure of the decision tree needs to inherit and expand from previous iterations. Thus, the results at a node are correlated and comparable between iterations. In addition, the tree is designed flexibly

so that the global optimal solution can be quickly found in each iteration. To achieve both stability and flexibility of the tree, we develop the dynamic task and processor selection policies in the following sections, which are applied to the undiscovered portion of the search space in iterations.

3) *Dynamic Task Selection*: The DBB algorithm travels through the decision tree to find the optimal solution by constantly updating the current solution with better ones. All the branches with no better solutions will be pruned without traveling. Thus, the sooner a better solution (i.e., the solution is close to the optimal one) is found, the more sub-spaces of the tree are pruned without traveling. Hence, it significantly reduces the solving time.

The tasks in $\tilde{\Phi}$ always need to be offloaded to satisfy their requirements, whereas a proportion of tasks in $\hat{\Phi}$ may not be offloaded due to ENs' resource limitation. Thus, in the DBB, the tasks in $\tilde{\Phi}$ will be chosen before the ones in $\hat{\Phi}$. Besides, the tasks with higher energy benefits per resource requirement unit are likely offloaded to ENs/cloud in the optimal solution. Thus, in each group, i.e., $\tilde{\Phi}$ and $\hat{\Phi}$, these tasks will be early chosen at nodes close to the root of the decision tree.

From Eq. (10), we can determine the maximum benefits of task I_i among all possible offloading decision solutions as $\Delta_i^{max} = \max_{\mathbf{x}_i} \{\Delta_i\}$. Then, from Eqs. (9) and (10), we have

$$\Delta_i^{max} = \begin{cases} E_i^l - \min_{j \leq (M+1)} \{E_{ij}^f\}, & I_i \in \hat{\Phi}, \\ \max_{j \leq (M+1)} \{E_{ij}^f\} - \min_{j \leq (M+1)} \{E_{ij}^f\}, & I_i \in \tilde{\Phi}. \end{cases} \quad (31)$$

For simplicity, we assume that the delays of tasks mostly belong to the computation. Let $r_i^{min} = \frac{L_i^u w_i}{t_i^c - \zeta}$ be a lower bound of computation resource required by task I_i . We then define the rate of benefits as $rate_i = \frac{\Delta_i^{max}}{r_i^{min}}$.

For each UE n with the task set Φ_n ($1 \leq n \leq N$), let Φ_n^+ be the set of tasks chosen at the ancestors of the current node. Let Φ^* be the set of N tasks with the highest rate $rate_i$ from N UEs. We have

$$\Phi^* = \{I_n \mid I_n = \operatorname{argmax}_{I_i \in \Phi_n / \Phi_n^+} rate_i, \forall n \leq N\}. \quad (32)$$

Here, the computational task I_{i^*} will be selected if it can help to increase the utility function most. Thus, the selection of task I_{i^*} can be determined as follows:

$$\begin{aligned} I_{i^*} &= \operatorname{argmax}_{I_i \in \Phi^*} (\rho_i \ln(u_n^+ + \Delta_i^{max}) - \rho_i \ln(u_n^+)) \\ &= \operatorname{argmax}_{I_i \in \Phi^*} \rho_i \ln \left(1 + \frac{\Delta_i^{max}}{u_n^+} \right), \end{aligned} \quad (33)$$

in which u_n^+ is the total utility of all tasks in Φ_n^+ .

4) *Balancing Processor Selection*: For a selected computational task I_{i^*} as in Section III-E3, we choose a processor (i.e., the UE, an EN, or the CS), aiming to balance the joint communication and computation load amongst ENs and the CS. Mathematically, this helps to create the most efficient subproblem Benders cuts at early iterations. Consequently, the optimal offloading solution satisfying the feasible resource allocation at all ENs can be found with a few iterations, thereby reducing the overall solving time. Besides, the delay

satisfaction rate as in Section III-C2 will be balanced and optimized amongst the tasks.

At the current node of the depth l of the decision tree, assume that task I_{i^*} is selected. We need to sort the possible processors (i.e., the UE, ENs, and the CS) towards task I_{i^*} in the ascending order of estimated delay. Let $\Phi_j^{t^*}$ and $\Phi_j^{s^*}$, respectively, be the temporary sets of chosen tasks being processed at EN j and the CS (via EN j). Let β_j^f and β_j^c be the upper bounds of the delay satisfaction rate of all tasks in $\Phi_j^{t^*+s^*}$ and I_{i^*} when they are executed at EN j and the CS (via EN j), respectively. We define these parameters as follows.

$$\beta_j^f = \left(\frac{\sum_{i \in \Phi_j^{t^*+s^*}} L_i^{u'} + L_{i^*}^{u'}}{R_j^u} + \frac{\sum_{i \in \Phi_j^{t^*+s^*}} L_i^{d'} + L_{i^*}^{d'}}{R_j^d} + \frac{\sum_{i \in \Phi_j^{t^*}} L_i^{u'} w_i' + L_{i^*}^{u'} w_{i^*}'}{R_j^f} \right), \forall j \in \mathbb{G}(q). \quad (34)$$

$$\beta_j^c = \left(\frac{\sum_{i \in \Phi_j^{t^*+s^*}} L_i^{u'} + L_{i^*}^{u'}}{R_j^u} + \frac{\sum_{i \in \Phi_j^{t^*+s^*}} L_i^{d'} + L_{i^*}^{d'}}{R_j^d} + \frac{\sum_{i \in \Phi_j^{t^*}} L_i^{c'} + L_{i^*}^{c'}}{\mathcal{B}_j} \right). \quad (35)$$

Here, $\mathbb{G}(q)$ is the set of all ENs that support the application type q .

Task I_{i^*} will be tried to offload to the processors in the order of $(F_1, \dots, C_1, \dots, L)$. $\beta_j^f \leq \beta_{j+1}^f$ and $\beta_j^c \leq \beta_{j+1}^c$, in which F_j , C_j and L , respectively, determine processors as EN j , the CS (via EN j), and the UE towards task I_{i^*} .

In Algorithm 1, the DBB is structured as a decision tree as in Section III-E1, then at every node on the tree, the most suitable task is selected for branching as in Section III-E3, then the branches from this node is developed according to the order of processors as in Section III-E4. To find the optimal offloading solution, the DBB algorithm travels through the tree between nodes via edges determined by the branches, using the incremental depth-first search as in Section III-E2. The proposed DBBD algorithm, which uses the DBB to solve the master problem, is introduced in Algorithm 2 as follows.

F. DBBD Algorithm

The DBBD algorithm, presented in **Algorithm 2**, finds the optimal solution by iteratively solving (\mathbf{MP}_0) and (\mathbf{SP}_1) . Initially, it initializes the iterator $k = 1$ and sets $cuts^{(k)}$ in (\mathbf{MP}_0) with $4(M+1)$ resource Benders cuts as in Section III-D2. Other prefixed-decision Benders cuts are also added to $cuts^{(k)}$ as in Section III-D3. At iteration (k) , the DBB algorithm finds $\mathbf{x}^{(k)} \in X_0$ of (\mathbf{MP}_0) satisfying $cuts^{(k)}$. With $\mathbf{x}^{(k)}$, $(M+1)$ problems of the form (\mathbf{SP}_1) with assigned

Algorithm 1: DBB Algorithm

Input : Set Φ of tasks $I_i (L_i^u, L_i^d, w_i, t_i^r, s_i^r, q, n)$
Set of M ENs $\{(R_j^u, R_j^d, R_j^f, s_j^f, \Psi_j)\}$
Set \mathcal{N} of UEs, Security levels \mathbb{S}
Application types \mathbb{Q} , Cloud server $(\mathcal{B}, \mathcal{C})$
Decision tree at k -th iteration $tree^{(k)}$

Output: Optimal $(\mathbf{x}^{(k)}, maxU)$ of (MP_0)
Decision tree for next iteration $tree^{(k+1)}$

```

1 begin
2    $(\mathbf{x}^{(k)}, maxU) \leftarrow (\emptyset, -\infty)$   $\triangleright$  Empty solution
3    $tree^{(k+1)}.empty()$   $\triangleright$  Empty tree for next iteration
4   if  $k = 1$  then  $tree^{(k)}.push((MP_0))$ 
5   while  $tree^{(k)}.isNotEmpty()$  do
6      $p \leftarrow tree^{(k)}.pop()$   $\triangleright$  Get (IP) from top of stack
7     if  $p$  was solved and its result is not better than
        $maxU$  then
8        $tree^{(k+1)}.push(\text{sub-tree from } p)$   $\triangleright$  Store all
        (IP) on sub-tree from  $p$  for next iteration
9       Prune sub-tree from  $p$  in  $tree^{(k)}$ 
10      continue  $\triangleright$  Skip  $p$  at current iteration
11       $(\tilde{\mathbf{x}}, subU) \leftarrow \text{Solve } (IP)$  of  $p$  then return its
        relaxed optimal solution and value
12      if  $\tilde{\mathbf{x}}$  is not found then
13        Prune sub-tree from  $p$  in  $tree^{(k)}$ 
14      else if  $subU \leq maxU$  then
15         $tree^{(k+1)}.push(\text{sub-tree from } p)$ 
16        Prune sub-tree from  $p$  in  $tree^{(k)}$ 
17      else if  $\tilde{\mathbf{x}}$  are integer then
18         $(\mathbf{x}^{(k)}, maxU) \leftarrow (\tilde{\mathbf{x}}, subU)$   $\triangleright$  Update
        solution and optimal result
19         $tree^{(k+1)}.push(\text{sub-tree from } p)$ 
20        Prune sub-tree from  $p$  in  $tree^{(k)}$ 
21      else if  $p$  was not branched then
22        Find task  $I_{i^*}$  and processors
         $(F_1^*, \dots, C_1^*, \dots, L)$  for  $I_{i^*}$  as in
        Sections III-E3 and III-E4
23         $list \leftarrow \text{Branch } p$  to create sub-tree of  $p$  by
        trying decisions of  $I_{i^*}$  in order
         $(F_1^*, \dots, C_1^*, \dots, L)$ 
24        for each  $chil$  in  $list$  do
25          Simplify  $chil$  as in Section III-E1.
26           $tree^{(k)}.push(chil)$   $\triangleright$  Put problem into
          stack
27        end
28         $tree^{(k+1)}.push(\text{sub-tree from } p)$   $\triangleright$  For next
        iteration
29      end
30    end
31  end
32  Return  $(\mathbf{x}^{(k)}, maxU)$  and  $tree^{(k+1)}$ 

```

tasks $\Phi_j^{s+t} \subseteq \Phi$ at $(M+1)$ ENs are defined. Then, using a convex solver, every EN j independently solves the variant of (SP_1) , i.e., (SP_2) , to find a resource allocation solution toward Φ_j^{t+s} . Before that, Theorem 3 can determine the feasibility of (SP_1) . If (SP_1) has no solution, a new Benders cut $c_j^{(k)}$ as in Section III-D1 will be updated into $cuts^{(k+1)}$ of (MP_0) for the later iterations. If $\mathbf{x}^{(k)}$ of (MP_0) does not exist, then DBBD can conclude the infeasibility of (P_0) . With $\mathbf{x}^{(k)}$ of (MP_0) , if $(M+1)$ problems of the form (SP_1) have solutions $(\mathbf{r}, \mathbf{b}) = (\{\mathbf{r}_j\}, \{\mathbf{b}_j\})$, then DBBD can conclude $(\mathbf{x}^{(k)}, \mathbf{r}, \mathbf{b})$ is the optimal solution of (P_0) .

In Algorithm 2, Theorem 3 is used to check the feasibility of (SP_1) before calling the solver. Additionally, by using Theorem 4, the resource cutting-planes are created at the initial stage of (MP_0) . Thus, the subproblems violating Theorem 4 are prevented during the iterations. As a result, the computation time of the DBBD algorithm can be remarkably reduced.

Algorithm 2: DBBD Algorithm

Input : Set Φ of tasks $I_i (L_i^u, L_i^d, w_i, t_i^r, s_i^r, q, n)$
Set of $(M+1)$ ENs $\{(R_j^u, R_j^d, R_j^f, s_j^f, \Psi_j)\}$
Set \mathcal{N} of UEs, Security levels \mathbb{S}
Application types \mathbb{Q} , Cloud server $(\mathcal{B}, \mathcal{C})$

Output: Optimal $(\mathbf{x}, \mathbf{r}, \mathbf{b})$ of (P_0)

```

1 begin
2    $k \leftarrow (k+1)$ ,  $cuts^{(k)} \leftarrow \bigcup_{j=1}^{M+1} \{c_j^u, c_j^d, c_j^f, c_j^b\}$ .
3   while solution  $(\mathbf{x}, \mathbf{r}, \mathbf{b})$  has not been found do
4      $\mathbf{x} \leftarrow \text{DBB algorithm solve } (MP_0)$  with
        $cuts^{(k)}$ .  $\triangleright$   $\mathbf{x}$  stores  $\mathbf{x}^{(k)}$  at iteration  $k$ 
5     if  $\mathbf{x}$  is found then
6       Solution  $\mathbf{x}$  defines  $(M+1)$  problems
         $(SP_1)$  with assigned tasks  $\Phi_1^{t+s}, \dots, \Phi_{M+1}^{t+s}$ .
7     else Return Problem  $(P_0)$  is infeasible.
8     for  $(j = 1; j \leq M+1; j = j+1)$  do
9        $(\mathbf{r}_j, \mathbf{b}_j) \leftarrow \text{Solver solves } (SP_1)$  at EN  $j$ 
        with assigned tasks  $\Phi_j^{t+s}$ .
10      if  $(\mathbf{r}_j, \mathbf{b}_j)$  is not found then
11        Update new cut  $c_j^{(k)}$  into  $cuts^{(k+1)}$ .
12      end
13      if  $(\mathbf{r}, \mathbf{b}) = (\{\mathbf{r}_j\}, \{\mathbf{b}_j\})$  is found then
14        Optimal  $(\mathbf{x}, \mathbf{r}, \mathbf{b})$  has been found.
15         $k \leftarrow (k+1)$   $\triangleright$  For next iteration
16      end
17    end
18  end
19  Return  $(\mathbf{x}, \mathbf{r}, \mathbf{b})$ 

```

G. Complexity Analysis

In this section, we analyze the complexity of the DBBD w.r.t. the number of tasks and edge nodes.

1) *Size of Original Problem:* With $(M+1)$ ENs including the cloud server V , the original problem (P_0) has $4(M+1)$ resource constraints for $(C_2), (C_3), (C_4)$, and (C_5) described in Eq. (17). In addition, to formulate each task I_i in (P_0) , we need to consider $(2(M+1)+1)$ binary and $4(M+1)$

real variables, together with three constraints for the delay, offloading, and security as shown in (\mathcal{C}_1) , (\mathcal{C}_6) and (\mathcal{C}_7) . The constraints (\mathcal{C}_8) and (\mathcal{C}_9) in Eq. (18) fix the offloading variables, and thus they are not counted here. Therefore, with $|\Phi|$ tasks and $(M+1)$ edge nodes, the original problem (\mathbf{P}_0) has respectively $|\Phi|(2(M+1)+1)$ integer and $4|\Phi|(M+1)$ real variables, and $(3|\Phi|+4(M+1))$ constraints including $|\Phi|$ for the offloading decisions, $|\Phi|$ for the security requirements, $|\Phi|$ for the delay requirements of the tasks and $4(M+1)$ for the resource requirements of ENs and the cloud as described in Eqs. (17) and (18). Thus, the relaxed problem $(\bar{\mathbf{P}}_0)$ of (\mathbf{P}_0) has totally $|\Phi|(6(M+1)+1)$ real variables and $(3|\Phi|+4(M+1))$ constraints.

2) *Size of Problems in DBBD*: For the DBBD algorithm, the master problem (\mathbf{MP}_0) and $(M+1)$ subproblems of the form (\mathbf{SP}_2) are iteratively solved. At iteration k , (\mathbf{MP}_0) is an integer problem with $|\Phi|(2(M+1)+1)$ binary offloading variables and at most $(2|\Phi|+4(M+1)+k(M+1))$ constraints including $2|\Phi|$ for the offloading decision and security requirements as (\mathcal{C}_5) and (\mathcal{C}_7) described in Eq. (18), $4(M+1)$ for resource Benders cuts as in Section III-D2, and at most $k(M+1)$ for the subproblem Benders cuts from solving $(M+1)$ subproblems k times as in Section III-D1. Furthermore, each subproblem (\mathbf{SP}_2) is assigned an average of $|\Phi|/(M+1)$ tasks. Thus, it has approximate $4|\Phi|/(M+1)$ resources allocation variables and $(|\Phi|/(M+1)+4)$ constraints including $|\Phi|/(M+1)$ for the delay of $|\Phi|/(M+1)$ tasks as (\mathcal{C}_{1j}) in Eq. (24) and 4 constraints for the resources requirements at the edge node as (\mathcal{C}_{2j}) , (\mathcal{C}_{3j}) , (\mathcal{C}_{4j}) , and (\mathcal{C}_{9j}) described in Eq. (24). In the worst case, (\mathbf{SP}_2) is assigned all $|\Phi|$ tasks, and thus it has at most $4|\Phi|$ resources allocation variables and $(|\Phi|+4)$ constraints. However, if this big subproblem violates the resources constraints at the edge node according to Theorem 4, it will not be created due to the generation of resource Benders cuts as in Section III-D2.

3) *Complexity of DBBD*: With $|\Phi|$ tasks and M ENs, there are $M^{|\Phi|+1}$ possible problems of the form (\mathbf{SP}_1) with the task numbers increasing from 0 to $|\Phi|$ and $M^{|\Phi|}$ master problems (\mathbf{MP}_0) . Thus, in the worst situation, the DBBD algorithm has complexity in the order of $O(M^{|\Phi|})$. However, with the support of Benders cut generations, most of the useless subproblems are excluded. Consequently, in practice, the solving time is far less than that of the worst case. This is also because (\mathbf{MP}_0) and (\mathbf{SP}_1) have linear sizes over the number of tasks.

IV. PERFORMANCE EVALUATION

A. Fairness Metrics

In edge computing systems, a large number of UEs/tasks often interacts and shares the same communication and computation resources of ENs and the CS. Thus, We will study how the numbers of UEs/tasks and the percentage of available resources at ENs affect the fairness, energy benefits, and total consumed energy of all UEs. The work [24] used the envy-free index (EF) to evaluate the fairness of game-based problems. However, the EF index is only suitable for the resource allocation problems that are formed as multi-agent

problems. In this paper, the problem is formulated as an MINLP, thus we will use Jain's index and min-max ratio to capture the fairness [27]. These indexes are defined as $\text{Jain's index} = \frac{(\sum_{n=1}^N u_n)^2}{N \sum_{n=1}^N u_n^2}$ and $\text{Min-Max ratio} = \frac{\min_{n \leq N} \{u_n\}}{\max_{n \leq N} \{u_n\}}$ where u_n is the utility function of devices n as in Eq. (13).

B. Experiment Setup

We adopt the configuration of the Nokia N900 for all UEs as presented in [34]. Each UE has CPU rate $f_i^l = 1$ Giga cycles/s and the CPU power consumption rate P_i^l modelled by parameters $(\alpha, \gamma) = (10^{-11} \text{ Watt/cycle}^2, 2)$ as in [28]–[30]. The transmitting and receiving energy configuration of the connection between UEs and ENs are based on either the 3G near connection or WLAN connection of the Nokia N900 as in Table 2 in [34]. For the 3G near connections, the energy consumption units to transmit and receive, respectively, are $e_{ij}^u = 0.658$ J/Mb and $e_{ij}^d = 0.278$ J/Mb. For the WLAN connections, the energy consumption for transmitting and receiving a unit are lesser and vary in ranges, $e_{ij}^u = [0.071, 0.213]$ J/Mb and $e_{ij}^d = [0.071, 0.213]$ J/Mb, respectively. These parameters are equivalent to the range from 0.5 to 1.5 times of standard values (i.e., 0.142 J/Mb and 0.142 J/Mb) described in Table 2 in [34]. In this work, all devices have the same weight $\rho_n = 1$, which shows that they are considered equally and fairly. UEs have computational tasks of 5 application types $\mathcal{Q} = \{1, \dots, 5\}$ under 3 security levels $\mathcal{S} = \{1(\text{High}), 2(\text{Medium}), 3(\text{Low})\}$. Based on the computational task of face recognition application as in [30], we then generate computational tasks $I_i(L_i^u, L_i^d, w_i, t_i^r, s_i^r, q, n)$ ($I_i \in \Phi$) are generated as $L_i^u = 1$ MB, $L_i^d = 0.1$ MB, $w_i = 5$ Giga cycles/Mb, $t_i^r = 5$ s, $s_i^r \in \mathcal{S}$, and $q \in \mathcal{Q}$. Three ENs have the uplink and downlink capacity in the range [11, 110] Mbps, which surrounds 72 Mbps, the highest WiFi theoretical physical-layer data rate of 802.11n smartphones [35], [36]. Besides, while each EN can randomly support only 3 application types, the CS can support every application type in \mathcal{Q} . We set $B_j = 100$ Mbps for the backhaul capacity between ENs and the CS. The CS often have to serve a large number of tasks, thus we assume that each task can get the maximum 5 Mbps of the backhaul rate. Additionally, the cloud server allocates $C_q = 10$ Giga cycles/s to each task of application type q that is forwarded via ENs. Other parameters are given in Table III. Different settings are provided in specific experiment scenarios.

Our proposed framework, i.e., DBBD, is compared with the total utility maximization framework, e.g., FFBD, where the total energy consumption is minimized without considering the fairness [2]. This policy is also called the social welfare maximization scheme (SWM) in [23], [24]. The DBBD and the benchmark, i.e., FFBD, are implemented using the **MOSEK** Optimizer API [37]. To highlight other performance (i.e., load balance and average delay) of the DBB algorithm that helps the DBBD in solving the MP, we implement two Benders decomposition variants of the FFBD, namely FFBD-I and FFBD-B. The FFBD-I uses the default linear **MOSEK** integer solver to solve the MP, whereas FFBD-B solves the

TABLE III: Experimental parameters

Parameters	Value
Number of UEs N	2 – 12
Number of ENs M	3
Number of computation tasks $ \Phi $	2 – 24
CPU rate of UEs f_i^t	1 Giga cycles/s
Security level of UEs s_i^t	1(High)
Energy consumption model of UEs (α, γ)	$(10^{-11} \text{ Watt/cycle}^2, 2)$
Unit transmitting energy consumption to ENs e_{ij}^u	0.071 – 0.213 J/Mb 0.658 J/Mb
Unit receiving energy consumption from ENs e_{ij}^d	0.071 – 0.213 J/Mb 0.278 J/Mb
Application type $q \in \mathbb{Q}$	$\mathbb{Q} = \{1, \dots, 5\}$
Processing rate of each EN R_j^f	1.5 – 15 Giga cycles/s
Uplink data rate of each EN R_j^u	11 – 110 Mbps
Downlink data rate of each EN R_j^d	11 – 110 Mbps
Security level of each EN $s_j^f \in \mathbb{S}$	$\mathbb{S} = \{1, \dots, 3\}$
CPU rate of cloud $\mathcal{C} = \{C_1, \dots, C_Q\}$	$\{10, \dots, 10\}$ Giga cycles/s
Backhaul capacity between FNs and cloud $\mathcal{B} = \{B_1, \dots, B_M\}$	$\{100, \dots, 100\}$ Mbps
Upper bound of backhaul rate	$b_{ij} \leq 5$ Mbps
Security level of cloud towards application $q: s_q^c \in \mathbb{S}$	$\mathbb{S} = \{1, \dots, 3\}$
Multi-access delay ζ	20ms

MP using a standard branch-and-bound method without the load balancing implementation. In the FFBD-B, computational tasks are offloaded to EN j as much as possible before EN $j + 1$. In the DBBD and FFBD, the minimum and maximum energy benefits of UEs are denoted by DBBD^{\min} , DBBD^{\max} and FFBD^{\min} , FFBD^{\max} , respectively. We compare different schemes using the same data sets and capture the main trends in the figures.

C. Numerical Results

For the case the edge computing systems can process only a proportion of tasks, we design three scenarios, i.e., Scenarios IV-C1, IV-C2, and IV-C3, to study how different parameters affect the fairness. For the case the systems have enough resources to process all tasks, we design only one scenario, i.e., Scenario IV-C4. In the first three scenarios, the offload demand is higher than the abilities of ENs. Thus, the load balance amongst ENs will not be investigated since all ENs get the maximum load. Similarly, we will not analyze the average delay since the offloaded tasks are allocated just enough resources to meet their delay requirements.

1) Scenario IV-C1 - Varying the Number of Devices:

In this scenario, we investigate the effect of the number of UEs on the fairness, energy benefits, and total energy consumption of all UEs. Three ENs with WLAN connections are configured with total resources $(\sum R_j^u, \sum R_j^d, \sum R_j^f) = (108 \text{ Mbps}, 108 \text{ Mbps}, 15 \text{ Giga cycles/s})$ so that they can process $50\% \times 24 = 12$ computational tasks. Then, we vary the number of UEs N from 2 to 12 with unit uplink/downlink energy consumption increase by 0.01 J/Mb from 0.071 J/Mb to 0.213 J/Mb. Consequently, these devices will have different energy consumption rates for their offloaded tasks. To evaluate the fairness of these schemes, each device is set an equal demand with $24/N$ tasks for each experiment. We also set

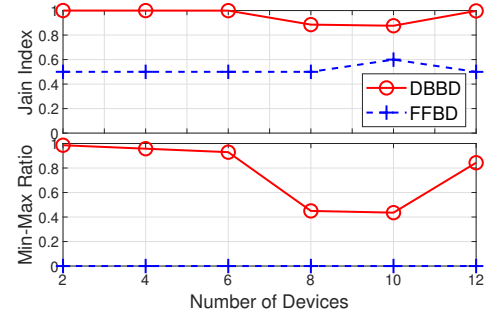
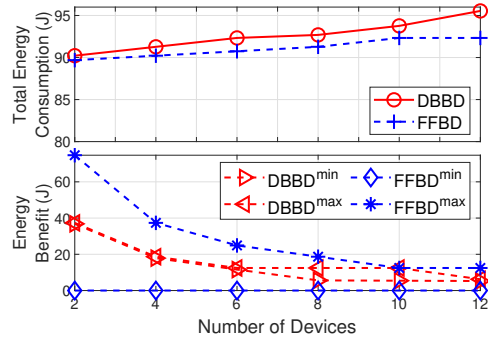


Fig. 3: J the num

Fig. 4: Total consumed energy and energy benefits as the number of devices N is increased.

application compatibility and the highest security level 1 for all ENs and devices so that they can process tasks. By these settings, all tasks get energy benefits from offloading and these tasks can be processed either locally or at ENs satisfying their requirements. Other parameters are set as in Table III.

Figs. 3 and 4, respectively, show the fairness indexes and the energy benefits of mobile devices for the proposed methods when the number of devices N is increased from 2 to 12. In Fig. 3, we can observe that both the Jain's index and min-max ratio in the DBBD algorithm are much higher than those in the benchmark FFBD algorithm. Especially, both indexes are close to their maximum value of 1 for the cases of 2, 4, 6, and 12 devices in the DBBD. This is because the DBBD aims to maximize the proportionally fair energy benefits. Consequently, each device has an equal number of offloaded tasks, i.e., 6, 3, 2, and 1, respectively, for these cases. We recall that there is a total of 12 offloaded tasks as described in the scenario's settings. For the cases of 8 and 10 devices, some of them have 1 offloaded task while others have 2, and consequently, the Jain's index and min-max ratio in these cases are lower than other cases' for the DBBD algorithm. The FFBD algorithm minimizes the total consumed energy, equivalently maximizes the total energy benefits of devices. Noticeably, in the scenario's settings, the transmitting/receiving energy consumption units of device $n + 1$ are 0.01 J/Mb higher than those of device n . Consequently, in the FFBD algorithm, 12 tasks of devices with less energy consumption are offloaded, whereas 12 tasks of devices with higher energy consumption are processed locally. Thus, the Jain's index of the FFBD algorithm is mostly close to 0.5 and

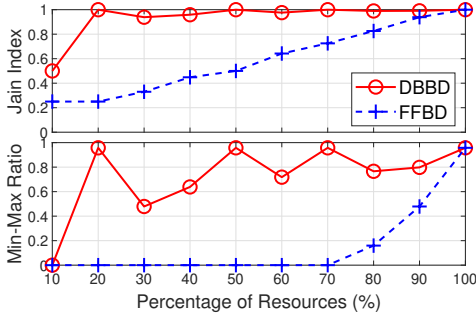


Fig. 5: J
the edge

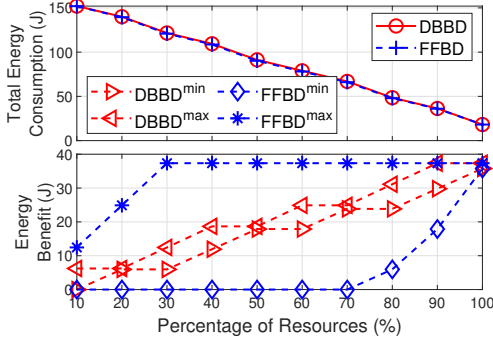


Fig. 6: Total consumed energy and energy benefits as the edge nodes' resources are increased.

the min-max ratio is 0 for all experiments.

The fairness and efficiency of the proposed method are also demonstrated in Fig. 4 in terms of the total energy consumption of all UEs and the energy benefits per device. Although the total energy consumption of the FFBD is a little lower than that of the DBBD, the gap between the minimum (FFBD^{\min}) and maximum (FFBD^{\max}) energy benefits of the FFBD is bigger than that of the DBBD (DBBD^{\min} and DBBD^{\max}). This is because the FFBD tries to minimize the total consumed energy, whereas the DBBD algorithm aims to maximize the fairness in terms of energy benefits. The energy benefits of each device also match the trends of fairness indexes in both methods. The zero value of the minimum energy benefits (FFBD^{\min}) also shows that all the tasks of some devices are processed locally in the FFBD.

2) *Scenario IV-C2 - Varying Edge Nodes' Resources:* Here, we study how the available resources of ENs affect the fairness, energy benefits, and total energy consumption of all devices. We keep the experiment of 4 devices in Scenario IV-C1, in which each device has 6 tasks. We then vary the total resources of 3 ENs ($\sum R_j^u, \sum R_j^d, \sum R_j^f$) from (21.6 Mbps, 21.6 Mbps, 3 Giga cycles/s) to (216 Mbps, 216 Mbps, 30 Giga cycles/s) so that the edge computing can support from 10% to 100% of tasks.

Figs. 5 and 6, respectively, show the fairness indexes and the energy benefits of UEs for the schemes when the available resources of ENs are increased. From Fig. 5, we can observe that both the Jain's index and min-max ratio in the DBBD are much higher than those in the benchmark, i.e., FFBD.

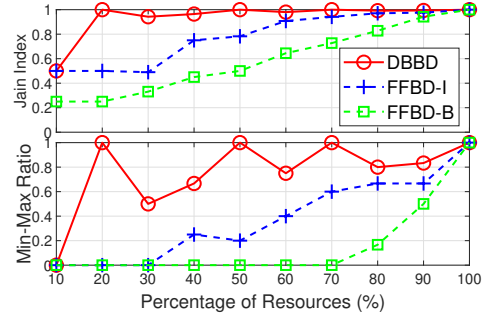


Fig. 7: Jain's index and Min-Max Ratio of energy benefits as the edge nodes' resources are increased while devices' configurations are the same.

Especially, in the DBBD, the Jain's index is close to 1 in all experiments except the case the amount of resources is only enough for 10% of tasks. This is because the more resources the ENs have, the more tasks the UEs can offload. In the DBBD, these offloaded tasks are distributed equally among UEs to gain the fairness. For example, when the ENs can support processing $60\% \times 24 = 14$ tasks, the 4 UEs have respectively 4, 4, 3, and 3 offloaded tasks. As a result, the Jain's index is close to the maximum value of 1, and the min-max ratio is close to 0.75. Similar to Scenarios IV-C1, in the FFBD, the UEs with more energy efficiency from offloading have offloaded tasks, whereas other UEs process their tasks locally. Thus, the Jain's index of the FFBD is increased from around 0.25 to 1 and its min-max ratio is 0 for most experiments. For example, when the edge computing can support 60%, i.e., 14 tasks, 4 UEs have, respectively, 6, 6, 2, and 0 offloaded tasks (i.e., all 6 tasks of UE 4 are processed locally). In this case, the Jain's index is around 0.64, and the min-max ratio is 0 when all tasks of UE 4 are processed locally.

As in Scenario IV-C1, Fig. 6 shows that the energy consumption of FFBD is a little lower than that of the DBBD. The energy benefit of each device also matches the trends of fairness indexes in both schemes. Especially, while the gap between the minimum (DBBD^{\min}) and maximum (DBBD^{\max}) energy benefits of the DBBD is quite small, the gap of the FFBD is very large for most experiments. This is because only the tasks of devices with less communication energy consumption units are offloaded in the FFBD.

3) *Scenario IV-C3 - Varying Edge Nodes' Resources and Setting the same Devices' Configurations:* The settings in this scenario are similar to Scenario IV-C2 except for the transmitting/receiving energy consumption units between UEs and ENs are the same as 0.071 J/Mb. In other words, all devices get the same energy benefits from offloading any computational task. We investigate how three different schemes, i.e., DBBD and FFBD-I/B, return their solutions when the optimal offloading solution may not be unique.

In Fig. 7, we can observe that the index patterns of the DBBD are similar to those in Scenario IV-C2. This is because the DBBD maximizes the proportional fairness, which is not affected much by a little difference in the energy benefits of UEs. However, Fig. 7 shows that the FFBD-I and FFBD-B

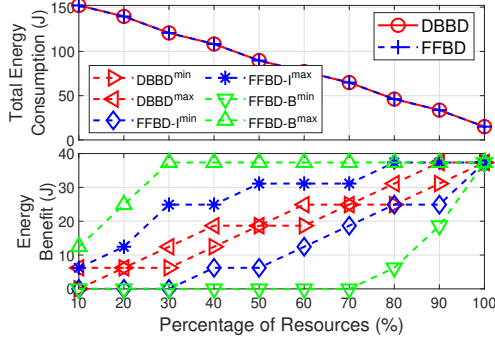


Fig. 8: Total consumed energy and energy benefits as the edge nodes' resources are increased while devices' configurations are the same.

return different solutions, though they solve the same problem minimizing total consumed energy. This is because the default MOSEK integer solver in the FFBD-I returns any arbitrary offloading solution for the MP, whereas the standard branch-and-bound algorithm in the FFBD-B tries to offload the tasks of UE n as much as possible before offloading the tasks of UE $n + 1$. Thus, the Jain's index and min-max ratio of the FFBD-B are the smallest in the three schemes.

In Fig. 8, the three schemes, i.e., DBBD and FFBD-I/B, have the same energy consumption, but their maximum and minimum energy benefits between UEs are different. Particularly, the gap between the minimum (FFBD-B^{min}) and maximum (FFBD-B^{max}) energy benefits of the FFBD-B is bigger than that of the FFBD-I, and the gap of the DBBD (between DBBD^{min} and DBBD^{max}) is the smallest. From this scenario, we can conclude that when an integer problem has some optimal solutions, only the DBBD with the proposed DBB algorithm for the master problem can return the optimal one satisfying the fairness amongst devices.

4) *Scenario IV-C4 - Varying the Number of Tasks:* In this scenario, we study how the number of tasks affects the fairness, energy benefits, and total energy consumption of all UEs. At first, two devices have an equal number of tasks $|\Phi|/2$. We then vary the total number of tasks $|\Phi|$ from 2 to 24. The two devices have WLAN connections to ENs 1 and 2, and the 3G near connections to EN 3. The WLAN uplink/downlink energy consumption units, respectively, are 0.071 J/Mb and 0.081 J/Mb. The 3G uplink and downlink energy consumption units, respectively, are 0.658 J/Mb and 0.278 J/Mb for both devices. ENs 1 and 2 with WLAN connections have resources (108 Mbps, 108 Mbps, 15 Giga cycles/s). Thus, these ENs have enough resources to process 24 computational tasks. EN 3 with the 3G near connections has resources (72 Mbps, 72 Mbps, 10 Giga cycles/s). We set application compatibility and the highest security level 1 for all ENs and UEs so that tasks can be processed either locally or at ENs. Other parameters are set as in Table III.

From Fig. 9, the Jain's index and min-max ratio of both the FFBD and DBBD are approximately equal to 1 when the number of tasks is increased. Similarly, Fig. 10 shows that the DBBD and FFBD have the same total energy consumption and maximum/minimum energy benefits for all experiments.

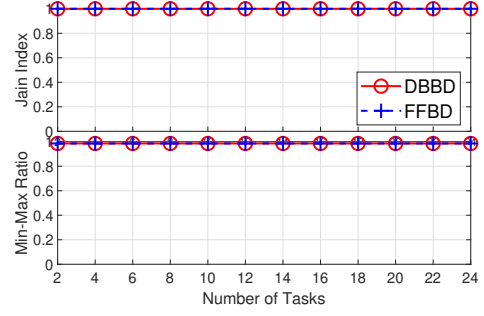


Fig. 9: Jain's index and Min-Max Ratio of energy benefits as the num

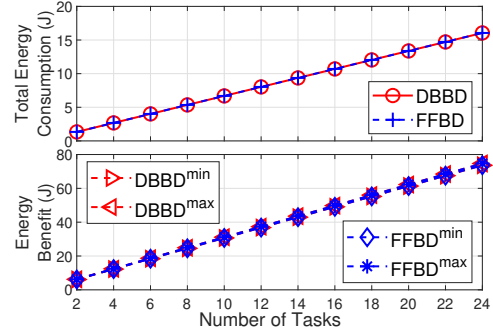


Fig. 10: Total consumed energy and energy benefits as the number of tasks is increased.

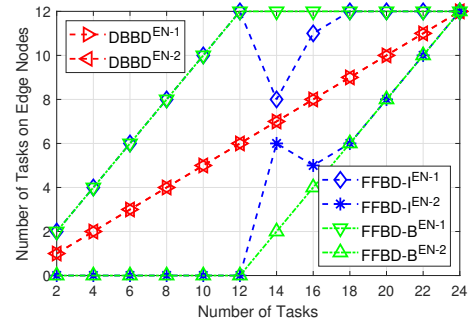


Fig. 11: Number of tasks offloaded to each edge node as the number of tasks is increased.

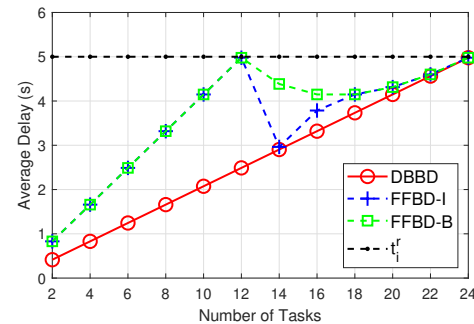


Fig. 12: Average delay of tasks as the number of tasks is increased.

These are because when the ENs have sufficient resources to process all tasks, all UEs get the maximum energy benefits, whatever scheme (i.e., DBBD or FFBD) is used. These benefits are equal since all UEs have the same configuration and the number of tasks.

Figs. 11 and 12 show the number of tasks offloaded to each edge node and the average delay of all tasks. From Fig. 11, the DBBD algorithm offloads tasks equally to edge nodes 1 and 2 (labeled DBBD^{EN-1} and DBBD^{EN-2}). This is because of the load balance implementation in the DBB algorithm for the master problem. The FFBD-I algorithm returns an arbitrary offloading decision due to the usage of default solver, whereas the FFBD-B algorithm returns the solution in which tasks are offloaded priority to the edge node 1 and then to edge node 2. Take the experiment with 16 tasks as an example, the DBBD, FFBD-I, and FFBD-B algorithms, respectively, offload (8, 8), (11, 5), and (12, 4) tasks to edge nodes-1 and 2. As a result, the DBBD algorithm has a lower average delay than the FFBD-I/B algorithms have as in Fig. 12.

V. CONCLUSION

We have considered the fairness among user devices in the joint task offloading and resource allocation problem for the multi-layer cooperative edge computing network. To that end, we have formulated a proportional fairness maximization problem that turns out to be NP-hard. To find its optimal solution, we have developed a dynamic branch-and-bound Benders decomposition algorithm (DBBD) to decompose the original problem into subproblems that can be solved parallelly at edge nodes. We have also developed a dynamic branch-and-bound method (DBB), which can solve the master problem with low complexity and satisfy the load balance between edge nodes. We then have compared the DBBD method with some benchmarks, namely FFBD-I/B, that optimize the energy consumption without fairness consideration. Numerical results showed that the DBBD always returns the optimal solution, which maximizes the proportional fairness in terms of energy benefits amongst user devices. The fairness metrics, i.e., the Jain's index and Min-Max ratio, also showed that the proposed scheme outperforms the benchmarks, i.e., FFBD-I/B.

APPENDIX A

PROOF OF THEOREM 1

Proof. First, we will show that the objective $\sum_{n=1}^N \rho_n \ln(u_n)$ is a concave function w.r.t. $(\mathbf{x}, \mathbf{r}, \mathbf{b})$. Obviously, the function $\ln(u_n)$ is concave w.r.t. (u_n) . From Eqs. (1), (3), (5), 7, (10), and (13), the utility u_n is a linear function of variables \mathbf{x} because $(E_i^{base} - \mathbf{e}_i)$ (i.e., in $u_n = \sum_{I_i \in \Phi_n} \Delta_i = \sum_{I_i \in \Phi_n} (E_i^{base} - \mathbf{e}_i)^\top \mathbf{x}_i$) is a constant vector. Consequently, $\ln(u_n)$ is a concave function w.r.t. $(\mathbf{x}, \mathbf{r}, \mathbf{b})$ according to the rule of composition with an affine mapping [25]. Due to $\rho_n > 0, \forall 1 \leq n \leq N$, we have $\sum_{n=1}^N \rho_n \ln(u_n)$ is a concave function w.r.t. $(\mathbf{x}, \mathbf{r}, \mathbf{b})$.

Second, we will show that all constraint functions in (\mathbf{R}_0) and $(\tilde{\mathbf{X}}_0)$ are convex. From Eqs. (2), (4), (6), (8), and (12), the delay $T_i = \mathbf{h}_i^\top \mathbf{y}_i$ is the sum of functions, i.e., $x_i^{l2}, \frac{x_{ij}^{f2}}{r_{ij}^u}, \frac{x_{ij}^{f2}}{r_{ij}^d}$,

$\frac{x_{ij}^{f2}}{r_{ij}^f}, x_{ij}^{c2}, \frac{x_{ij}^{c2}}{r_{ij}^u}, \frac{x_{ij}^{c2}}{r_{ij}^d}$, and $\frac{x_{ij}^{c2}}{b_{ij}} \forall j \in \mathcal{M}$, with positive coefficients, e.g., $\frac{L_i^u w_i}{r_{ij}^f}, L_i^u, L_i^d, (L_i^u w_i)$, and $(L_i^u + L_i^d)$. The function x^2 is convex. We need to prove that function $g(x, r) = \frac{x^2}{r}$ is convex. Let $\mathbf{H} = \nabla^2 g(x, r)$ be the Hessian of $g(x, r)$.

$$\mathbf{H} = \begin{bmatrix} \frac{\partial^2 g}{\partial x^2} & \frac{\partial^2 g}{\partial x \partial r} \\ \frac{\partial^2 g}{\partial r \partial x} & \frac{\partial^2 g}{\partial r^2} \end{bmatrix} = \begin{bmatrix} \frac{2}{r} & -\frac{2x}{r^2} \\ -\frac{2x}{r^2} & \frac{2x^2}{r^3} \end{bmatrix}. \quad (36)$$

Then, given an arbitrary real vector $\mathbf{v} = (v_1, v_2)$, we have

$$\begin{aligned} \mathbf{v}^\top \mathbf{H} \mathbf{v} &= v_1 \left(v_1 \frac{2}{r} - v_2 \frac{2x}{r^2} \right) + v_2 \left(-v_1 \frac{2x}{r^2} + v_2 \frac{2x^2}{r^3} \right), \\ &= \frac{2}{r} \left(v_1 - v_2 \frac{x}{r} \right)^2. \end{aligned} \quad (37)$$

The variable r in Eq. (37) is a representation of the resource allocation variables $r_{ij}^u, r_{ij}^d, r_{ij}^f, b_{ij} \geq 0$. Therefore, we have $r \geq 0$ and $\mathbf{v}^\top \mathbf{H} \mathbf{v} \geq 0$. In other words, \mathbf{H} is positive semidefinite, and thus $g(x, r)$ is convex w.r.t. (x, r) [25]. As a result, T_i is convex since it is the nonnegative weighted sum of convex functions. Particularly, the constraint (C_1) in (\mathbf{R}_0) is a convex function w.r.t. $(\mathbf{x}, \mathbf{r}, \mathbf{b})$. Besides, the constraints (C_{2-9}) in (\mathbf{R}_0) and $(\tilde{\mathbf{X}}_0)$ are linear functions.

Since the relaxed problem $(\tilde{\mathbf{P}}_0)$ aims to maximize the concave objective function over the feasible convex set, which is defined by (\mathbf{R}_0) and $(\tilde{\mathbf{X}}_0)$, the problem $(\tilde{\mathbf{P}}_0)$ is a convex optimization problem [25]. ■

APPENDIX B

PROOF OF THEOREM 2

Proof. We have $cuts^{(k)}$ and $cuts^{(k+1)}$, respectively, are the sets of Benders cuts of (\mathbf{MP}_0) at iterations (k) and $(k+1)$. At iteration k , we assume that (\mathbf{MP}_0) has a solution $\mathbf{x}^{(k)}$, which leads to at least one infeasible subproblem (\mathbf{SP}_1) . Consequently, a new subproblem Benders cut will be added to $cuts^{(k+1)}$, thus we have $cuts^{(k)} \subset cuts^{(k+1)}$. This leads to $\max_{\mathbf{x} \in \mathbf{X}_0} \{ \sum_{n=1}^N \rho_n \ln(u_n) \}$ s.t. $cuts^{(k)} \geq \max_{\mathbf{x} \in \mathbf{X}_0} \{ \sum_{n=1}^N \rho_n \ln(u_n) \}$ s.t. $cuts^{(k+1)}$. In other words, $\max_{\mathbf{x} \in \mathbf{X}_0} \{ \sum_{n=1}^N \rho_n \ln(u_n) \}$ s.t. $cuts^{(k)}$ is a decreasing function with iteration k . Thus, the first found solution $(\mathbf{x}, \mathbf{r}, \mathbf{b})$ of (\mathbf{MP}_0) and (\mathbf{SP}_0) is the optimal solution of (\mathbf{P}_0) .

If (\mathbf{MP}_0) has no solution at iteration k , it will not have any solution at subsequent iterations because $cuts^{(k)} \subset cuts^{(k+v)}, \forall v \geq 1$. Hence, we can conclude the unfeasibility of the original problem (\mathbf{P}_0) . ■

APPENDIX C

PROOF OF THEOREM 3

Proof. Consider the resource allocation $\mathbf{r}_{ij} = (r_{ij}^u, r_{ij}^d, r_{ij}^f, b_{ij}) = (\frac{L_i^{u'}}{\beta_{bal}^u}, \frac{L_i^{d'}}{\beta_{bal}^d}, \frac{L_i^{f'} w_i}{\beta_{bal}^f}, \frac{L_i^{c'}}{\beta_{bal}^c}), \forall i \in \Phi_j^{t+s}$ toward Task I_i . We have $\beta_i = \frac{L_i^{u'}}{r_{ij}^u} + \frac{L_i^{d'}}{r_{ij}^d} + \frac{L_i^{f'} w_i}{r_{ij}^f} + \frac{L_i^{c'}}{b_{ij}} = (\beta_{bal}^u + \beta_{bal}^d + \beta_{bal}^f + \beta_{bal}^c) = \beta_{bal}$. Here, $r_{ij}^f = 0$ and $\frac{L_i^{u'}}{r_{ij}^u} = 0, \forall i \in \Phi_j^s$, whereas $b_{ij} = 0$ and $\frac{L_i^{c'}}{b_{ij}} = 0, \forall i \in \Phi_j^t$. Thus, $\beta_i = \beta_{bal} \leq 1, \forall i \in \Phi_j^{t+s}$.

Besides, $\sum_{i \in \Phi_j^{t+s}} r_{ij}^u = R_j^u$, $\sum_{i \in \Phi_j^{t+s}} r_{ij}^d = R_j^d$, $\sum_{i \in \Phi_j^{t+s}} r_{ij}^f = R_j^f$, and $\sum_{i \in \Phi_j^{t+s}} b_{ij} = B_j$ satisfying the resource constraints at EN j . To conclude, (SP₁) is feasible with the resource allocation solution \mathbf{r}_{ij} . ■

APPENDIX D PROOF OF THEOREM 4

Proof. We first prove the following Lemma 1 to support Theorem 4.

Lemma 1. *Given two sequences of numbers $p_i \geq 0$, $q_i > 0$, $\forall i \in N$. We have $\max_{i \in N} \{\frac{p_i}{q_i}\} \geq \frac{\sum_{i \in N} p_i}{\sum_{i \in N} q_i}$.*

Proof. if $\frac{p_1}{q_1} \geq \frac{p_2}{q_2}$ then $\max\{\frac{p_1}{q_1}, \frac{p_2}{q_2}\} = \frac{p_1}{q_1} \geq \frac{p_1+p_2}{q_1+q_2}$. Otherwise, if $\frac{p_1}{q_1} < \frac{p_2}{q_2}$ then $\max\{\frac{p_1}{q_1}, \frac{p_2}{q_2}\} = \frac{p_2}{q_2} > \frac{p_1+p_2}{q_1+q_2}$. In other words, $\max\{\frac{p_1}{q_1}, \frac{p_2}{q_2}\} \geq \frac{p_1+p_2}{q_1+q_2}$. Similarly, $\max\{\frac{p_1+p_2}{q_1+q_2}, \frac{p_3}{q_3}\} \geq \frac{p_1+p_2+p_3}{q_1+q_2+q_3}$. Therefore, $\max\{\frac{p_1}{q_1}, \frac{p_2}{q_2}, \frac{p_3}{q_3}\} \geq \max\{\frac{p_1+p_2}{q_1+q_2}, \frac{p_3}{q_3}\} \geq \frac{p_1+p_2+p_3}{q_1+q_2+q_3}$. Repeatedly, we have $\max_{i \in N} \{\frac{p_i}{q_i}\} \geq \frac{\sum_{i \in N} p_i}{\sum_{i \in N} q_i}$. ■

Applying Lemma 1 into $\{L_{ij}^{u'}\}_{i \in \Phi_j^{t+s}}$ and $\{r_{ij}^u\}_{i \in \Phi_j^{t+s}}$, we have $\max_{i \in \Phi_j^{t+s}} \{\frac{L_{ij}^{u'}}{r_{ij}^u}\} \geq \frac{\sum_{i \in \Phi_j^{t+s}} L_{ij}^{u'}}{\sum_{i \in \Phi_j^{t+s}} r_{ij}^u}$. According to resource allocation conditions, $\sum_{i \in \Phi_j^{t+s}} r_{ij}^u \leq R_j^u$, we have $\max_{i \in \Phi_j^{t+s}} \{\frac{L_{ij}^{u'}}{r_{ij}^u}\} \geq \frac{\sum_{i \in \Phi_j^{t+s}} L_{ij}^{u'}}{R_j^u}$. Therefore, $\max_{i \in \Phi_j^{t+s}} \{\frac{L_{ij}^{u'}}{r_{ij}^u}\} > 1$. Without loss of

generality, we assume $\exists i^* \in \Phi_j^{t+s}$, $\frac{L_{i^*}^{u'}}{r_{i^*}^u} = \max_{i \in \Phi_j^{t+s}} \{\frac{L_{ij}^{u'}}{r_{ij}^u}\} > 1$. Consequently, $\beta_{i^*} = \left(\frac{L_{i^*}^{u'}}{r_{i^*}^u} + \frac{L_{i^*}^{d'}}{r_{i^*}^d} + \frac{L_{i^*}^{f'}}{r_{i^*}^f} + \frac{L_{i^*}^{c'}}{b_{i^*}} \right) > \frac{L_{i^*}^{u'}}{r_{i^*}^u} > 1$. It contradicts the delay requirement of Task I_{i^*} , $\beta_{i^*} \leq 1$ as in Eq. (27). Thus, the problem (SP₁) is infeasible.

Other cases, i.e., $\frac{\sum_{i \in \Phi_j^{t+s}} L_{ij}^{d'}}{R_j^d} > 1$, $\frac{\sum_{i \in \Phi_j^{t+s}} L_{ij}^{f'}}{R_j^f} > 1$, and $\frac{\sum_{i \in \Phi_j^{t+s}} L_{ij}^{c'}}{B_j} > 1$, are proved in a similar way. ■

APPENDIX E PROOF OF THEOREM 5

Proof. First, the objective γ_j is linear w.r.t. $(\mathbf{r}_j, \mathbf{b}_j, \gamma_j)$. Second, we need to show that all constraint functions in (RZ_j) are convex. From Eq. (27) and (C_{1j}) in Eq. (29), the delay constraint $\beta_i \leq \gamma_j$ can be rewritten as $\left(\frac{L_{ij}^{u'}}{r_{ij}^u} + \frac{L_{ij}^{d'}}{r_{ij}^d} + \frac{L_{ij}^{f'}}{r_{ij}^f} + \frac{L_{ij}^{c'}}{b_{ij}} \right) - \gamma_j \leq 0$. This function is the sum of convex functions, i.e., $\frac{1}{r_{ij}^u}$, $\frac{1}{r_{ij}^d}$, $\frac{1}{r_{ij}^f}$, $\frac{1}{b_{ij}}$, and $-\gamma_j$ with positive coefficients, e.g., $L_{ij}^{u'}$, $L_{ij}^{d'}$, $L_{ij}^{f'}$, $L_{ij}^{c'}$, and 1. Thus, the function $\left(\frac{L_{ij}^{u'}}{r_{ij}^u} + \frac{L_{ij}^{d'}}{r_{ij}^d} + \frac{L_{ij}^{f'}}{r_{ij}^f} + \frac{L_{ij}^{c'}}{b_{ij}} \right) - \gamma_j$ is convex w.r.t. $(\mathbf{r}_j, \mathbf{b}_j, \gamma_j)$. Besides, all other constraints in Eq. (29) are linear functions.

Since the subproblem (SP₂) aims to minimize the convex objective function over the feasible convex set, that is defined by (RZ_j), the subproblem (SP₂) is a convex optimization problem [25]. ■

REFERENCES

- [1] P. Mach and Z. Becvar, "Mobile edge computing: A survey on architecture and computation offloading," *IEEE Communications Surveys & Tutorials*, vol. 19, no. 3, pp. 1628–1656, 2017.
- [2] T. T. Vu, D. N. Nguyen, D. T. Hoang, E. Dutkiewicz, and T. V. Nguyen, "Optimal energy efficiency with delay constraints for multi-layer cooperative fog computing networks," *IEEE Transactions on Communications*, vol. 69, no. 6, pp. 3911–3929, 2021.
- [3] Y. Mao, C. You, J. Zhang, K. Huang, and K. B. Letaief, "A survey on mobile edge computing: The communication perspective," *IEEE Communications Surveys & Tutorials*, vol. 19, no. 4, pp. 2322–2358, 2017.
- [4] H. El-Sayed, S. Sankar, M. Prasad, D. Puthal, A. Gupta, M. Mohanty, and C. Lin, "Edge of things: The big picture on the integration of edge, iot and the cloud in a distributed computing environment," *IEEE Access*, vol. 6, pp. 1706–1717, 2018.
- [5] M. Chen, B. Liang, and M. Dong, "Multi-user multi-task offloading and resource allocation in mobile cloud systems," *IEEE Transactions on Wireless Communications*, vol. 17, no. 10, pp. 6790–6805, 2018.
- [6] M. Chen, M. Dong, and B. Liang, "Resource sharing of a computing access point for multi-user mobile cloud offloading with delay constraints," *IEEE Transactions on Mobile Computing*, vol. 17, no. 12, pp. 2868–2881, 2018.
- [7] J. Du, L. Zhao, J. Feng, and X. Chu, "Computation offloading and resource allocation in mixed fog/cloud computing systems with min-max fairness guarantee," *IEEE Transactions on Communications*, vol. 66, no. 4, pp. 1594–1608, 2018.
- [8] J. Du, L. Zhao, X. Chu, F. R. Yu, J. Feng, and I. C, "Enabling low-latency applications in lte-a based mixed fog/cloud computing systems," *IEEE Transactions on Vehicular Technology*, vol. 68, no. 2, pp. 1757–1771, 2019.
- [9] H. Xing, L. Liu, J. Xu, and A. Nallanathan, "Joint task assignment and resource allocation for d2d-enabled mobile-edge computing," *IEEE Transactions on Communications*, vol. 67, no. 6, pp. 4193–4207, 2019.
- [10] C. Liu, M. Bennis, M. Debbah, and H. V. Poor, "Dynamic task offloading and resource allocation for ultra-reliable low-latency edge computing," *IEEE Transactions on Communications*, vol. 67, no. 6, pp. 4132–4150, 2019.
- [11] T. X. Tran and D. Pompili, "Joint task offloading and resource allocation for multi-server mobile-edge computing networks," *IEEE Transactions on Vehicular Technology*, vol. 68, no. 1, pp. 856–868, 2019.
- [12] J. Wang, K. Liu, B. Li, T. Liu, R. Li, and Z. Han, "Delay-sensitive multi-period computation offloading with reliability guarantees in fog networks," *IEEE Transactions on Mobile Computing*, pp. 1–1, 2019.
- [13] K. Kumar and Y. H. Lu, "Cloud computing for mobile users: Can offloading computation save energy?" *Computer*, vol. 43, no. 4, pp. 51–56, April 2010.
- [14] Y. Wang, X. Tao, X. Zhang, P. Zhang, and Y. T. Hou, "Cooperative task offloading in three-tier mobile computing networks: An admm framework," *IEEE Transactions on Vehicular Technology*, vol. 68, no. 3, pp. 2763–2776, 2019.
- [15] J. Wang, J. Hu, G. Min, A. Y. Zomaya, and N. Georgalas, "Fast adaptive task offloading in edge computing based on meta reinforcement learning," *IEEE Transactions on Parallel and Distributed Systems*, vol. 32, no. 1, pp. 242–253, 2021.
- [16] J. Wang, J. Hu, G. Min, W. Zhan, A. Zomaya, and N. Georgalas, "Dependent task offloading for edge computing based on deep reinforcement learning," *IEEE Transactions on Computers*, pp. 1–1, 2021.
- [17] J. Liu, K. Xiong, D. W. K. Ng, P. Fan, Z. Zhong, and K. B. Letaief, "Max-min energy balance in wireless-powered hierarchical fog-cloud computing networks," *IEEE Transactions on Wireless Communications*, vol. 19, no. 11, pp. 7064–7080, 2020.
- [18] G. Zhang, F. Shen, Z. Liu, Y. Yang, K. Wang, and M. Zhou, "Femto: Fair and energy-minimized task offloading for fog-enabled iot networks," *IEEE Internet of Things Journal*, vol. 6, no. 3, pp. 4388–4400, 2019.
- [19] Y. Dong, S. Guo, J. Liu, and Y. Yang, "Energy-efficient fair cooperation fog computing in mobile edge networks for smart city," *IEEE Internet of Things Journal*, pp. 1–1, 2019.
- [20] F. Li, H. Yao, J. Du, C. Jiang, Z. Han, and Y. Liu, "Auction design for edge computation offloading in sdn-based ultra dense networks," *IEEE Transactions on Mobile Computing*, pp. 1–1, 2020.
- [21] H. Liao, Y. Mu, Z. Zhou, M. Sun, Z. Wang, and C. Pan, "Blockchain and learning-based secure and intelligent task offloading for vehicular fog computing," *IEEE Transactions on Intelligent Transportation Systems*, vol. 22, no. 7, pp. 4051–4063, 2021.

- [22] Y. Zuo, S. Jin, and S. Zhang, "Computation offloading in untrusted mec-aided mobile blockchain iot systems," *IEEE Transactions on Wireless Communications*, vol. 20, no. 12, pp. 8333–8347, 2021.
- [23] D. T. Nguyen, L. B. Le, and V. Bhargava, "Price-based resource allocation for edge computing: A market equilibrium approach," *IEEE Transactions on Cloud Computing*, vol. 9, no. 1, pp. 302–317, 2021.
- [24] D. T. Nguyen, L. B. Le, and V. K. Bhargava, "A market-based framework for multi-resource allocation in fog computing," *IEEE/ACM Transactions on Networking*, vol. 27, no. 3, pp. 1151–1164, 2019.
- [25] S. Boyd and L. Vandenberghe, *Convex optimization*. Cambridge university press, 2004.
- [26] P. M. Narendra and K. Fukunaga, "A branch and bound algorithm for feature subset selection," *IEEE Transactions on computers*, no. 9, pp. 917–922, 1977.
- [27] R. K. Jain, D.-M. W. Chiu, and W. R. Hawe, "A quantitative measure of fairness and discrimination," *Eastern Research Laboratory, Digital Equipment Corporation, Hudson, MA*, 1984.
- [28] X. Lin, Y. Wang, Q. Xie, and M. Pedram, "Task scheduling with dynamic voltage and frequency scaling for energy minimization in the mobile cloud computing environment," *IEEE Transactions on Services Computing*, vol. 8, no. 2, pp. 175–186, 2015.
- [29] X. Chen, "Decentralized computation offloading game for mobile cloud computing," *IEEE Transactions on Parallel and Distributed Systems*, vol. 26, no. 4, pp. 974–983, 2015.
- [30] X. Chen, L. Jiao, W. Li, and X. Fu, "Efficient multi-user computation offloading for mobile-edge cloud computing," *IEEE/ACM Transactions on Networking*, vol. 24, no. 5, pp. 2795–2808, 2016.
- [31] Y. Wen, W. Zhang, and H. Luo, "Energy-optimal mobile application execution: Taming resource-poor mobile devices with cloud clones," in *2012 Proceedings IEEE INFOCOM*, Conference Proceedings, pp. 2716–2720.
- [32] F. P. Kelly, A. K. Maulloo, and D. K. H. Tan, "Rate control for communication networks: shadow prices, proportional fairness and stability," *Journal of the Operational Research Society*, vol. 49, no. 3, pp. 237–252, 1998. [Online]. Available: <https://doi.org/10.1057/palgrave.jors.2600523>
- [33] Y. Yu, X. Bu, K. Yang, and Z. Han, "Green fog computing resource allocation using joint benders decomposition, dinkelbach algorithm, and modified distributed inner convex approximation," in *2018 IEEE International Conference on Communications (ICC)*, Conference Proceedings, pp. 1–6.
- [34] A. P. Miettinen and J. K. Nurminen, "Energy efficiency of mobile clients in cloud computing," *HotCloud*, vol. 10, pp. 4–4, 2010.
- [35] F. Liu, E. Bala, E. Erkip, M. C. Beluri, and R. Yang, "Small-cell traffic balancing over licensed and unlicensed bands," *IEEE Transactions on Vehicular Technology*, vol. 64, no. 12, pp. 5850–5865, 2015.
- [36] S. K. Saha, P. Deshpande, P. P. Inamdar, R. K. Sheshadri, and D. Koutsoukolas, "Power-throughput tradeoffs of 802.11n/ac in smartphones," in *2015 IEEE Conference on Computer Communications (INFOCOM)*, Conference Proceedings, pp. 100–108.
- [37] E. D. Andersen and K. D. Andersen, "The mosek documentation and api reference," Report, 2019. [Online]. Available: <https://www.mosek.com/documentation/>